New Phytologist

Research

Xylem endophytes of *Salicaceae*: potential role in mitigating disease symptoms from *Xylella fastidiosa* or *Brenneria salicis*

Lena Pesenti[1], Salomé Lengrand[1], Alexandra Kahn[1,2], Louis Michot[1], François Marchandise[3], Cyril Focant[3], Sophie Richet[4], Frédéric Debode[4] and Claude Bragard[1]

[1]Earth and Life Institute - Applied Microbiology, Université Catholique de Louvain (UCLouvain), Louvain-la-Neuve, 1348, Belgium; [2]Department of Environmental Science, Policy, and Management, University of California Berkeley (UC Berkeley), 94720 Berkeley, USA; [3]Corder asbl, 1348, Louvain-la-Neuve, Belgium; [4]Life Sciences Department, Biological Engineering Unit, Walloon Agricultural Research Centre (CRA-W), 5030, Gembloux, Belgium

Authors for correspondence:
Lena Pesenti
Email: lena.pesenti@uclouvain.be

Claude Bragard
Email: claude.bragard@uclouvain.be

Received: *15 January 2026*
Accepted: *18 March 2026*

New Phytologist (2026) **251:** 455–476
doi: 10.1111/nph.71230

Key words: amplicons, *Bacillus*, *Erwinia*, isolation, metabarcoding, *Paraburkholderia*, *Pseudomonas*, xylem-limited pathogen.

Summary

- Increasing pressure from xylem-limited pathogens has driven the search for beneficial xylem-inhabiting endophytes that can enhance growth, stress tolerance, and disease resistance in woody plants. This study characterized the culturable xylem microbiota of *Salicaceae* species (willow and poplar) and evaluated their potential as biological control agents against vascular pathogens.
- A combination of microbial isolation, metabarcoding, and whole-genome sequencing was used to characterize xylem-associated bacteria. Functional traits were assessed through *in vitro* assays, while genome mining identified genes linked to plant-beneficial activities. Interactions between endophytes and pathogens were tested using fluorescently labeled strains in tobacco (*Nicotiana tabacum*) and *in vitro*-grown willow (*Salix caprea*).
- Bacterial genera (*Bacillus*, *Pseudomonas*, *Erwinia*) exhibited plant growth-promoting traits and strong antagonism against bacterial and fungal vascular pathogens, including *Xylella fastidiosa*, *Brenneria salicis*, *Fusarium spp*., and *Verticillium dahliae*. Genome analyses revealed functions related to nutrient acquisition, biofilm formation, and antimicrobial production. Co-inoculation assays significantly reduced pathogen load and disease symptoms in tobacco and mitigated symptoms in willow.
- Xylem endophytes act as context-dependent allies in woody plant defence. This study provides a functional and genomic framework supporting microbiome-based strategies to enhance resistance against vascular pathogens in long-lived woody hosts.

Introduction

Plants are considered as complex holobionts hosting microbial communities influencing their health, and resilience to environmental stress (Compant *et al*., 2024; Lengrand *et al*., 2024). This paradigm shift revealed that endophytes play critical roles in nutrient acquisition, growth, and stress mitigation, positioning them as key allies for plant against vascular pathogens (Yadeta & Thomma, 2013). On the other side, bacteria infecting the plant vascular system are among the most destructive, shutting down the plant's water and nutrient supply, leading to wilting and, to the death of the entire plant (Vinatzer *et al*., 2012). Xylem-specialized plant pathogenic bacteria share a distinctive ability to multiply and move systemically within the xylem, often without causing obvious symptoms (Purcell & Hopkins, 1996; Bragard *et al*., 2019a, 2019b). These pathogens are particularly difficult to manage due to their internal localization, systemic spread, and lack of effective curative treatments (Vinatzer, 2012; Yadeta & Thomma, 2013; De La Fuente *et al*., 2022). Hence, attention has increasingly turned to the plant microbiome for biocontrol and plant health promotion. Indeed, xylem harbors diverse microbial communities capable of influencing both plant physiology and immunity (Zicca *et al*., 2020; Anguita-Maeso *et al*., 2021), via resource competition, niche exclusion, or the production of antimicrobial compounds (Compant *et al*., 2005a, 2005b; Hardoim *et al*., 2015). Understanding the diversity and function of xylem-resident endophytes represents a crucial step toward developing microbiome-informed strategies for managing vascular diseases (Giampetruzzi *et al*., 2020).

To this extent, *Xylella fastidiosa* and *Brenneria salicis* have been selected as models for xylem-limited bacterial pathogens, given their distinct biology, ecological relevance, and increasing impact across Europe. Indeed, *X. fastidiosa* is a highly adaptable, quarantine-listed pathogen notoriously difficult to manage due to its ability to establish asymptomatic infections (Pesenti, 2025). Among potential model systems to investigate xylem endophytes with disease-mitigating functions, the *Salicaceae* family stands out as especially relevant. Recent work by Casarin *et al*. (2022) demonstrated that several *Salicaceae* species (*Salix alba*, *Salix caprea*,

Populus canescens, *P. tremula*) are susceptible to colonization by *X. fastidiosa*, even under temperate conditions, with systemic spread reaching stems and roots highlighting their potential role as asymptomatic reservoirs. By contrast, *B. salicis* primarily affects willow species, mainly *S. alba* and its complex but also *Salix fragilis* and *S. caprea*, and causes watermark disease, yet often persists as a harmless endophyte (Turner *et al.*, 1992; Maes *et al.*, 2009; Pesenti, 2024). Studying these two pathogens in the context of their interactions with the native xylem microbiome offers an unparalleled framework to uncover microbial-mediated mechanisms of disease suppression and host resilience. *Salicaceae* species naturally host complex and functionally diverse xylem microbiomes, making them an ideal system to explore how resident endophytes might modulate pathogen behavior or suppress symptom development. Their ecological distribution across Europe and frequent association with xylem-feeding insect vectors further support their use as an underexplored reservoir for vascular microbiome research (Casarin *et al.*, 2023). Studies have highlighted that endophytes isolated from *willows and poplars* exhibit potent antifungal activities, particularly against key soil- and xylem-invading pathogens such as *Fusarium oxysporum*, *F. culmorum*, and *Verticillium dahliae* (Guleria *et al.*, 2022; Zhang *et al.*, 2022; Doty *et al.*, 2023), offering a sustainable alternative to fungicides for vascular wilt diseases. Previous work has also demonstrated the biocontrol potential of *Paraburkholderia phytofirmans* PsJN against *X. fastidiosa* in grapevine (Baccari *et al.*, 2019).

By combining a cultivation-based and metabarcoding approach, we aimed to better characterize the bacterial communities associated with xylem sap in *Salicaceae*. Over 400 endophytic bacterial strains were isolated from xylem sap. Such isolates were screened for plant-beneficial traits, focusing on antagonistic activity against key xylem-invading pathogens. A selected subset of strains inhibiting *X. fastidiosa* and *B. salicis*, as well as vascular fungi such as *Fusarium* spp. and *V. dahlia*, underwent whole-genome sequencing and functional annotation to elucidate genetic determinants of biocontrol potential and adaptation to the xylem niche. In order to visualize and follow these strains within plant xylem vessels, three were tagged with fluorescent proteins, for direct visualization of their colonization, and interactions with pathogens within plant xylem vessels additionally to quantitative polymerase chain reaction (qPCR) quantification in tobacco and *in vitro*-grown willow (Andreote *et al.*, 2006; Casarin *et al.*, 2022).

By linking host plant identity to microbiome composition and functional potential, this study provides insights into the xylem-resident microbiota of willow and poplar and assesses the capacity of selected endophytic strains to limit colonization and symptom development by *X. fastidiosa* and *B. salicis* in complementary plant systems. This work identifies promising bacterial candidates for microbiome-based disease management strategies in woody plants.

Materials and Methods

Sampling of willows and poplars

Populus canescens (Aiton) Sm., *P. tremula* L. (1 + 0 – grown during one season without subsequent transplanting; Vloethemveld origin), *P. nigra* L., *Salix alba* L. (90/120 cm height class; 'Liempde'), *S. caprea* L. and *S. fragilis* L. plants were provided by ©Sylva Van Hulle nursery (Belgium). The plants were potted and kept in an insect-proof glasshouse (22°C day, 20°C night, 80% RH).

Xylem sap extraction for isolation and molecular identification of endophytic bacteria

For the culture-dependent approach, xylem sap of eight plants per species was collected at two-time points with a Scholander pressure chamber (Alexou & Peuke, 2013). To minimize contamination, a 2-cm stem segment was debarked and surface-sterilized. Pressure (35 bars) was applied until xylem sap emerged, and the first droplets were discarded to reduce external contamination (Anguita-Maeso *et al.*, 2020). For each plant, 50 µl of sap was plated in duplicate on Buffered Charcoal Yeast Extract (BCYE), Tryptic Soy Agar (TSA), King's B (KB), and Potato Dextrose Agar (PDA) media and incubated at 28°C for 2–3 d. Isolates were purified and stored at −80°C. Genomic DNA was extracted by heat lysis, and 16S rRNA genes were amplified with primers 27f/1492r (Weisburg *et al.*, 1991), Sanger-sequenced (Microsynth®), and identified by BLASTn against core_nt.

Xylem sap extraction for metabarcoding analysis

Based on preliminary tests, centrifugation was selected as the most efficient method to obtain sufficient xylem sap for metabarcoding analyses. Xylem sap from six plants per species was extracted by centrifuging 1.5-cm surface-sterilized branch segments for 20 min at 16 000 ***g***. DNA was extracted using Wizard Genomic DNA Purification Kit (Promega). DNA quality and concentration were verified using a NanoDrop spectrophotometer and a Qubit fluorometer (ThermoFisherScientific, Waltham, MA, USA). Given the low quantity of xylem sap, a two-step amplification strategy was employed. Near full-length bacterial 16S rRNA gene fragments were amplified (27f/1492r) (Weisburg *et al.*, 1991) and purified with Agencourt AMPure XP beads (Beckman Coulter, Danvers, MA, USA). Purified amplicons served as templates for region-specific amplification targeting V1–V3 region (27f/534r) and V3–V4 (341f/805r). Resulting amplicons were used for libraries preparation and sequenced on an Illumina MiSeq platform (Inview Microbiome pipeline, Eurofins®, Ebersberg, Germany). Extraction blanks and PCR negatives showed no detectable DNA and therefore were not sequenced (more information can be found in Supporting Information). Reads were deposited in the NCBI Sequence Read Archive under BioProject accession PRJNA1377930.

Bioinformatics and statistical analysis

Illumina MiSeq reads were demultiplexed and trimmed, then processed in RSTUDIO (v.4.4.1) using DADA2 (v.1.32). Reads were truncated to 240/200 bp (V1V3) and 260/220 bp (V3V4). Reads were denoised, merged, and chimera-filtered to generate an amplicon sequence variant (ASV) table. Taxonomy was

assigned using KRAKEN2 (v.2.1.3) against the GTDB database (r220) applying the default bootstrap confidence threshold (50). Samples with > 70% plant-derived reads were excluded. Alpha (ASV richness, Shannon) and beta (Bray–Curtis, PCoA) diversity analyses were used to assess community composition across hosts and primer pairs.

Confrontation assay to test antagonist activity against *X. fastidiosa* and *B. salicis*

The antagonistic activity of endophytic bacteria against *X. fastidiosa* KLN59.3 (Newman *et al.*, 2003 – provided by Steven E. Lindow – UC Berkeley) and *B. salicis* LMG2698 (Hauben *et al.*, 1998) was evaluated using dual-culture assays. In a 9-cm plate, three parallel rows of *X. fastidiosa* 20 µl drops (10^8 CFU ml^{-1}) were spotted; the middle row was flanked at each end by a 5 µl spot (10^8 CFU ml^{-1}) of endophytes the next day. Control plates were spotted with *X. fastidiosa* and a sterile media drop at ends. Inhibition was evaluated after 7–10 d. For *B. salicis*, 30 µl of pathogen suspension (10^8 CFU ml^{-1}) was spread on TSA and followed with 5 µl endophyte spots. The presence of inhibition halo or reduction in bacterial lawn density was assessed after 1–3 d at 28°C.

In vitro test investigating plant growth-promoting traits (PGPT) and antagonistic traits against pathogens

The 47 endophytes showing inhibition activity in the confrontation assay were tested for the following *in vitro* tests: phosphate solubilization, production of siderophores, swarming and swimming motility, indole-related compound production, and biofilm formation (O'Toole, 2010; Louden *et al.*, 2011; Baldan *et al.*, 2015; Paul & Sinha, 2017; Thomloudi *et al.*, 2021).

Fifteen strains (*B. cereus* 9–163, *B. mycoides* 8–62, *B. pseudomycoides* 7–2, 8–70, *B. subtilis* 9–155, *Bacillus velezensis* 3–53, 7–9, 9–143, 9–153, *B. wiedmannii* 9–170, *Erwinia rhapontici* 11–25, 12–58, *P. coleopterorum* 9–161, 9–174, *Pseudomonas graminis* 9–169), selected based on their *in vitro* score and the prevalence of occurrence in isolation, were used for an *in vitro* confrontation with four fungi associated with *Salicaceae* (*F. oxysporum* (MUCL3159), *F. culmorum* (MBC7956), *F. avenaceum* (MBC9248), and *V. dahliae* (MUCL14206); Doty *et al.*, 2023; Guleria *et al.*, 2022; Zhang *et al.*, 2022). Fungal plugs, cultivated on PDA for 3–4 d, were placed on plates with two drops of 10 µl of overnight bacterial culture (10^8 CFU ml^{-1}) and incubated at 22°C for 5 d. Fungal inhibition was assessed by measuring radial growth 5 d post inoculation and compared with control plates.

Genome sequencing and mining

The genome of the 15 strains has been sequenced. Genomic DNA was extracted using the Wizard Genomic DNA Purification Kit (Promega), purified with AMPure XP beads. Libraries were prepared and sequenced by Eurofins® using the Oxford Nanopore Technology (ONT) Lite Bacterial Genome Sequencing pipeline. Raw reads were deposited in NCBI under BioProject accession PRJNA1377930. Sequences were uploaded to the Type (Strain) Genome Server (TYGS; https://tygs.dsmz.de – accessed on 21 June 2024; Meier-Kolthoff *et al.*, 2013). Genomic relatedness was determined using average nucleotide identity (ANI) values computed with EzBioCloud (Yoon *et al.*, 2017). To evaluate the strain's potential for secondary metabolite production, genome mining was conducted using AntiSMASH (Blin *et al.*, 2023) and the virulence factor database (VFDB) with VFanalyser (Liu *et al.*, 2022). Functional pathways were identified using the Kyoto Encyclopedia of Genes and Genomes (KEGG, Moriya *et al.*, 2007; Ogata *et al.*, 1999). Plant growth-promoting traits (PGPT) were predicted using the PGPT-Pred module of PLaBAse v.1.01 from the annotated protein files for each strain using the BlastP+HMMER Aligner/Mapper (Patz *et al.*, 2021). PIFAR-BASE was used to identify 'plant bacterial only interaction factors' from the annotated protein files for each strain using the BlastP+HMMER Aligner/Mapper (Patz *et al.*, 2021).

Tagging phytopathogenic and endophytic strains with fluorescent protein

Overnight cultures of *B. salicis* LMG2698, *Escherichia coli* WM3064::Tn*7* mNeonGreen, and *E. coli* WM3064::pTNS*3* were centrifuged, resuspended in 2 ml of $MgCl_2$ (10 mM), and optical density (600 nm; OD600) was adjusted to 1, then mixed in a ratio of 1 and plated on TSA with diaminopimelic acid (DAP; 24 h, 28°C). Colonies were recovered and plated on TSA supplemented with gentamycin (10 µg ml^{-1}) and incubated (48 h, 28°C). The same protocol was applied to transform *E. rhapontici* 11–25 and 12–58 with *E. coli* WM3064::Tn*7* mCherry and *E. coli* WM3064::pTNS*3* (Choi & Schweizer, 2006).

Plasmids were obtained from an overnight liquid culture conducted in LB supplemented with spectinomycin and DAP (37°C, 220 rpm) of *E. coli* WM3064::Tn*7* mCherry and *E. coli* WM3064::pTNS*3*. Plasmid extraction was performed using the Spin miniprep kit (Qiagen). Competent cells (100 µl; Choi & Schweizer, 2006), washed three times in sucrose (300 mM), were electroporated (Gene Pulser, BioRad −2.5 kV, 25 µF, 200 Ω, 5 s) with 500 ng of each plasmid. After incubation (28°C, 220 rpm, 3 h), the transformed cells were plated on LBA supplemented with spectinomycin (25 µg ml^{-1}).

For all strains, fluorescence was evaluated under a confocal microscope. Plasmid insertion was verified by PCR (Supporting Information Table S1).

Inoculation and co-inoculation of tagged-endophytic strains and pathogens in *Nicotiana tabacum* and *Salix caprea in vitro* plantlets

Preparation of inocula Tobacco plants were used as model plants and *S. caprea in vitro* plantlets as model *Salicaceae*. The plants, not watered 2 d before and after the inoculation to boost intake, were kept in a temperate quarantine glasshouse (22°C day, 20°C night, 80%HR).

Bacterial inocula were prepared from colonies suspended in succinate–citrate–phosphate buffer (SCP, pH 7.0; EPPO, 2019). *X. fastidiosa* KLN59.3 was provided by Steve Lindow (UCBerkeley) and *P. phytofirmans* PsJN:: pIN29 by Lionel Moulin (IRD). For co-inoculation, suspension of one phytopathogenic and endophytic bacteria were mixed 1 : 1, with each strain at 10^8 CFU ml^{-1} in the final inoculum.

Plants were inoculated using the pinprick inoculation method (Hill & Purcell, 1995; Almeida *et al.*, 2001; Casarin *et al.*, 2022), applying three (tobacco) or one (willow) 10 µl drops of bacterial suspension (Casarin *et al.*, 2022).

Inoculation treatment Experiments were conducted in three independent inoculation series (Table 1).

Bacterial detection with PCR (T1) Main vein and petiole of the first leaf after the inoculation point and the apex leaf were tested by PCR at T1 (Table 1). DNA from main vein and petiole was extracted following a Cethyltrimethylammonium bromide (CTAB protocol (EPPO, 2019) then amplified by PCR. Primers sequences and PCR cycles are listed in Table S1, and plasmids sequences with annealing location in Fig. S1.

Bacterial detection with qPCR (Tf) Segments used for qPCR were homogenized in extraction bags (BIOREBA), and DNA was extracted using the CTAB method (EPPO, 2019). Target, primer sequences, and PCR conditions are provided in Table S2. Calibration parameters for all targets are provided in Fig. S2. qPCRs (20 µl) contained 2× Takyon SYBR MasterMix dTTP (Eurogentec, Herstal, Belgium), 500 nM primers, and 2 µl template DNA and were run in duplicate on a CFX96 thermocycler (Bio-Rad). Conversion of Cq values using target-specific standard curves yielded genome equivalent estimates consistent with relative Cq differences among treatments (Table S10).

Re-isolation (Tf) Re-isolation of inoculated bacteria was performed from the main vein of the first leaf after the inoculation point. Tissue was crushed in 1 ml SCP, plated on selective media, and incubated at 28°C for 1–10 d. Colonies of interest were detected by transillumination and confirmed by PCR (Table S1).

Bacterial detection with confocal microscopy (Tf) Bacterial colonization was visualized by confocal laser scanning microscopy. Transverse and longitudinal stem sections (*c.* 55 µm) from two stem segments were prepared using a microtome and observed with a STELLARIS confocal microscope (Leica Microsystems) using a water-immersion objective (20×/1.0NA). Fluorescently tagged bacteria were visualized using White Light Laser excitation and hybrid detectors with the following settings: GFP–488 nm; mNeon – 492 nm; mCherry and DsRed–561 nm. Transmitted light was simultaneously collected to visualize host tissue structure. Imaging parameters were kept constant across samples.

Statistical analyses Statistical analyses were performed in RSTUDIO (v.4.4.1). Final plant height and qPCR Cq values were analyzed using one-way ANOVA. When significant ($P < 0.05$), Tukey's HSD and compact letter displays were applied. Model assumptions were assessed by residual inspection. Further details are provided in Supporting Information.

Results

The study followed an approach from community characterization to functional validation. The xylem microbiome of six *Salicaceae* species was first analyzed using culture-dependent and metabarcoding methods, followed by functional prioritization to identify cultivable taxa with biocontrol potential. Selected candidates were then validated *in planta* in *N. tabacum* (model host) and *S. caprea* (woody *Salicaceae*), assessing xylem colonization, disease suppression, and pathogen DNA reduction under one- and three-month conditions.

Characterization of the *Salicaceae* xylem microbiome

The *Salicaceae* xylem microbiome was characterized using combined culture-dependent and metabarcoding approaches to capture cultivable bacteria and overall diversity, providing a basis for functional screening.

Culture-dependent approach To assess the culturable diversity of xylem-associated bacteria across Salicaceae hosts, eight plants per species from *P. canescens*, *P. tremula*, *P. nigra*, *S. alba*, *S. caprea*, and *S. fragilis* were sampled. Xylem sap was extracted using a Scholander pressure chamber and plated on BCYE, KB, TSA, and PDA selected to maximize recovery of phylogenetically diverse endophytes. In the culture-dependent approach, bacterial densities in xylem sap extracted with a Scholander pressure chamber ranged from 81 ± 5 to 563 ± 29 CFU ml^{-1} ($F = 5.988$; $P = 3.97e\text{-}05$), with plant species significantly affecting bacterial retrieval. BCYE yielded the highest counts (370 ± 28 CFU ml^{-1}), followed by KB (281 ± 24), TSA (280 ± 23), and PDA (144 ± 9).

A total of 4 phyla, 6 classes, 14 orders, 21 families, 43 genera, and 104 species were retrieved. The number of bacterial isolates recovered from xylem sap ranged from 41 to 111 among plant species ($F = 16.69$; $P = 1.17e\text{-}05$) and from 71 to 150 across culture media ($F = 16.59$; $P = 4.98e\text{-}05$; Fig. S3). The number of genera significantly depended on culture media and plant species ($P < 0.05$). Out of the total of 43 bacterial genera identified, 27 were detected in BCYE, 21 in PDA, 14 in KB, and 11 in TSA. Thirty-one bacterial species were identified in *S. alba*, 26 in *S. caprea*, 15 in *S. fragilis*, 49 in *P. canescens*, 30 in *P. tremula*, and 24 in *P. nigra*. Only five bacterial species were shared among the six *Salicaceae* species (core bacterial species: *B. velezensis*, *B. proteolyticus*, *B. toyonensis*, *B. tequilensis*, *B. subtilis*; Fig. S4). Six species were shared among the willow, and nine species among poplars (Fig. 1a).

Bacillota dominated the cultured community (78.0%), followed by *Pseudomonadota* (17.0%), *Actinomycetota* (4.8%), and *Bacteroidota* (0.2%). The most abundant genera were *Bacillus* (60.7%), *Pseudomonas* (9.5%), *Priestia* (5.0%), *Ralstonia*

Table 1 Inoculation were performed as three independent series: (i) November 2024 – inoculation of *Nicotiana tabacum* and *Salix caprea* with individual endophytic strains; (ii) December 2024 and April–May 2025 – 3 months of co-inoculations assay of pathogenic and endophytic bacteria; and (iii) September 2025 and November 2025 – 1-month co-inoculation assays of pathogenic and endophytic bacteria. T0 indicated the time of inoculation, T1 indicated the time of leaves collection for PCR detection and Tf the time of final harvest for confocal microscopy, isolation, and quantitative polymerase chain reaction detection. Values indicate the number of plants analyzed for each treatment and assay.

	Tobacco plants			Willow *in vitro* plantlets		
	Inoculation	Co-inoculation 1	Co-inoculation 2	Inoculation	Co-inoculation 1	Co-inoculation 2
T0	November 2024	December 2024	September 2025	November 2024	April–March 2025	November 2025
T1	November 2024 (2 wk)	February 2024 (1 month)	November 2025 (2 wk)	November 2024 (2 wk)	June 2025 (1 month)	December 2025 (2 wk)
Tf	December 2024 (1 month)	March-2025 (3 months)	October 2025 (1 month)	December 2024 (1 month)	July 2025 (3 month)	December 2025 (1 month)
Control	5	10	4	5	8	3
Brenneria velezensis 9–153	/	/	4	/	/	3
Erwinia rhapontici 11–25:: Tn*7* mCherry	10	10	4	10	8	3
Pseudomonas coleopterorum 9–161:: Tn*7* mCherry	10	10	4	10	8	3
Pseudomonas graminis 9–169:: Tn*7* mCherry	5	10	4	5	8	3
Paraburkholderia phytofirmans PsJN:: pIN29	5	10	4	5	8	3
Xylella fastidiosa KLN59.3	/	20	16	/	20	11
Xylella fastidiosa KLN59.3 + *B. velezensis 9–153*		/	16		/	11
Xylella fastidiosa KLN59.3 + *E. rhapontici* 11–25:: Tn*7* mCherry		20	16		20	11
Xylella fastidiosa KLN59.3 + *P. coleopterorum* 9–161:: Tn*7* mCherry		20	16		20	11
Xylella fastidiosa KLN59.3 + *P. graminis* 9–169:: Tn*7* mCherry		20	16		20	11
Xylella fastidiosa KLN59.3 + *P. phytofirmans* PsJN:: pIN29		20	16		20	11
Brenneria salicis LMG2698:: Tn*7* mNeon Green		20	16		20	11
B. salicis LMG2698:: Tn*7* mNeon Green + *B. velezensis 9–153*		/	16		/	11
B. salicis LMG2698:: Tn*7* mNeon Green + *E. rhapontici* 11–25:: Tn*7* mCherry		20	16		20	11
B. salicis LMG2698:: Tn*7* mNeon Green + *P. coleopterorum* 9–161:: Tn*7* mCherry		20	16		20	11
Brenneria salicis LMG2698:: Tn*7* mNeon Green + *P. graminis* 9–169:: Tn*7* mCherry		20	16		20	11
Brenneria salicis LMG2698:: Tn7 mNeon Green + *P. phytofirmans* PsJN:: pIN29		20	16		20	11

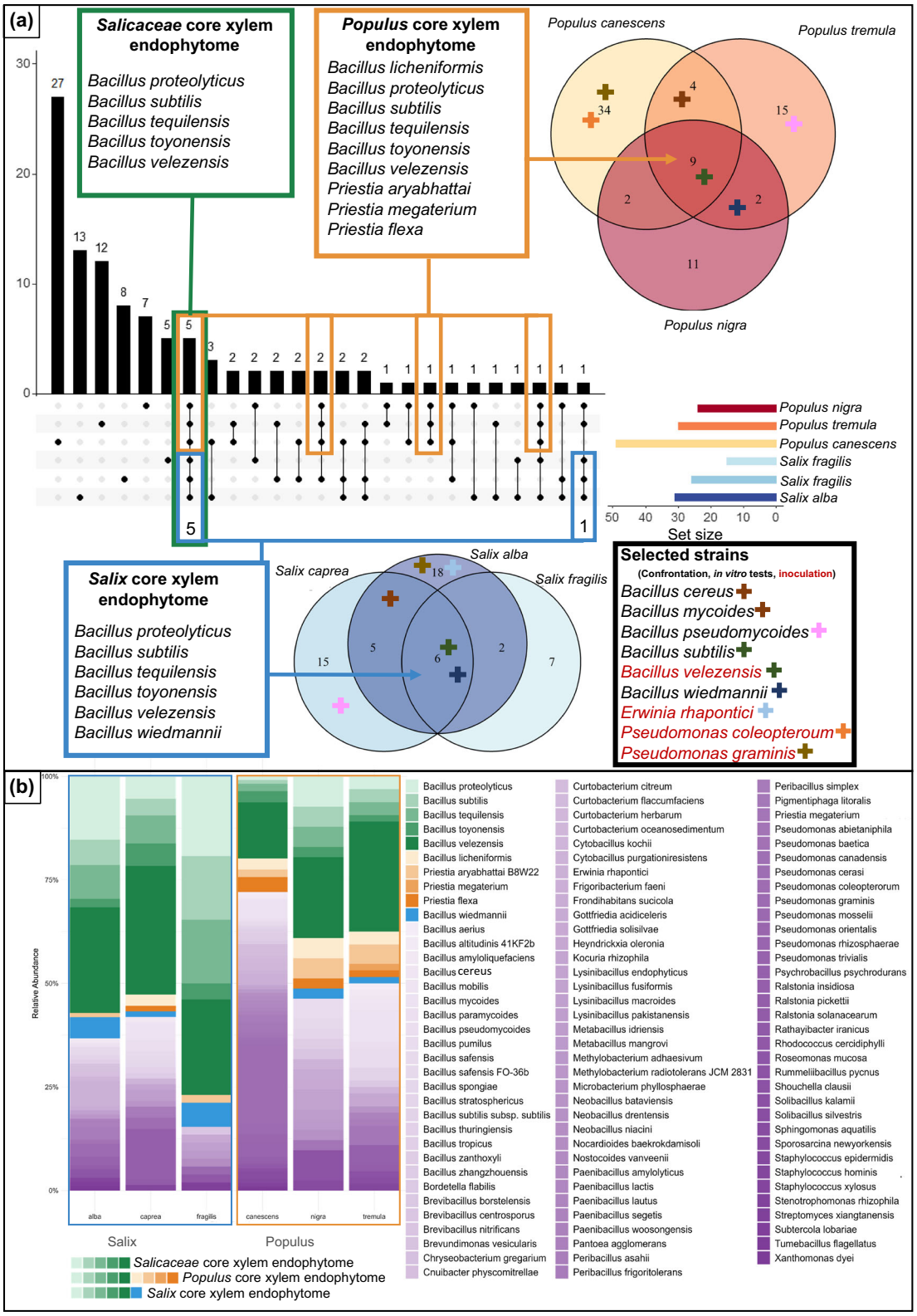

(3.0%), and *Curtobacterium* (1.8%). Despite some overlap, each plant species supports a distinct cultivated community, indicating that host identity shapes culturable bacterial diversity (Fig. 1b).

Bacterial diversity differed significantly among hosts, with richness from 6 (*S. caprea*) to 13.6 (*P. canescens*) and Shannon index from 1.24 to 2.00 (Kruskal–Wallis, $P \leq 0.0007$), poplars being more diverse than willows (Table S3).

Fig. 1 Bacterial species isolated from six *Salicaceae* species using culture-dependent methods. (a) Intersection of bacterial species distribution across *Salicaceae* host species:: *Populus canescens*, *Populus tremula*, *Populus nigra*, *Salix alba*, *Salix caprea*, and *Salix fragilis*. The set size (horizontal bars) represents the total number of bacterial species identified per host plant. The five species framed in green (*Bacillus proteolyticus*, *Bacillus velezensis*, *Bacillus toyonensis*, *Bacillus tequilensis*, *Bacillus subtilis*) were isolated from all six plant species. Blue and orange frame highlight species shared exclusively within willow and within poplar. The three willow species shared six species, while the three poplar species shared nine species, including *B. licheniformis*, *Priestia aryabhattai*, *P. megaterium*, and *P. flexa*. (b) Relative abundance of bacterial species isolated from six *Salicaceae* species using culture-dependent methods. Stacked barplots show the relative abundance of cultured bacterial species across individual host plant species: *S. alba*, *S. caprea*, *S. fragilis* (blue frame), *P. canescens*, *P. tremula*, and *P. nigra* (orange frame). Green genera shared by all six plant species, blue indicates genera common to the three willow species, and orange marks genera shared by the three poplar species. In the black frame, selection of representative endophytic strains used in subsequent experiments is indicated. Strains were selected based on their antagonistic activity against *Xylella fastidiosa* and *Brenneria salicis* in dual-culture assays, complemented by additional *in vitro* functional tests. Strains highlighted in red correspond to those further evaluated *in planta* through co-inoculation assays.

Culture-independent approach In the culture-independent approach, Illumina MiSeq yielded 2690 305 good-quality reads after the removal of chimeras, unassigned reads, and eukaryotic reads (Fig. S5).

A total of 1018 ASVs were identified across the four tree species, with similar proportions detected using the V1V3-27f/534r (452 ASVs, 44.4%) and V3V4-341f/805r (568 ASVs, 55.8%) primer sets. Both primer sets produced comparable community profiles, with minor differences in taxonomic depth. Alpha diversity (Chao1, Shannon) showed no significant differences among primers, plant genera, or species (Kruskal–Wallis, $P > 0.05$; Fig. S6).

A total of 13 phyla, 16 classes, 42 orders, 74 families, 158 genera, and 223 species were identified across the two PCR-primer pairs and the four *Salicaceae* species. The V3–V4 primers recovered more phyla than V1–V3 (13 vs 9), with similar trends at lower taxonomic levels. Nine phyla were shared, including dominant Pseudomonadota, Bacillota, and Actinomycetota. Fifteen genera were common to both primers across all hosts, defining the core microbiome. Poplars showed more diverse communities than willows, as illustrated at the genus level (Fig. 2).

Functional and genomic identification of candidate xylem allies

Following microbiome characterization, candidate endophytic strains with functional traits compatible with vascular biocontrol were identified through antagonism assays, PGPT screening, and genome sequencing to link phenotypic performance with genomic potential.

Confrontation assay to test antagonist activity against *X. fastidiosa* and *B. salicis* A total of 47 bacterial isolates and 26 different species exhibited antagonistic activity against one or both of the pathogenic bacteria strains under these conditions. These isolates belong to diverse genera, including *Bacillus*, *Priestia*, *Pseudomonas*, *Curtobacterium*, and *Stenotrophomonas*, known for their biocontrol potential (Fig. 4a).

In vitro* test investigating PGPT and antagonistic traits against pathogens and genome sequencing and mining** ***Functional diversity of antagonistic isolates. The 47 bacterial isolates exhibiting antagonistic activity were selected for further functional characterization to assess their potential plant-beneficial traits and to evaluate key features associated with plant–microbe and microbe–microbe interactions (Fig. 3). From those 47 isolates, 15 representative strains were selected for their superior performance and core-microbiome status to be tested against fungal pathogens.

Antifungal activity of selected endophytic strains. The 15 selected bacterial strains were evaluated against four major vascular fungal pathogens associated with woody hosts: *F. oxysporum*, *F. culmorum*, *F. avenaceum*, and *V. dahliae*. Antifungal activity was quantified by measuring fungal growth area in cm^2 5 d post inoculation, as compared to pathogen-only controls (Fig. 4b).

Broad inhibition was observed for *B. velezensis* (3–53, 9–143, 9–153) and *P. graminis* 9–169. Most other isolates showed selective activity against *Fusarium* spp. but little effect on *V. dahliae*, while *E. rhapontici* 11–25 and *P. coleopterorum* 9–174 showed no inhibition (Fig. 4b).

Genomic features, biocontrol-related traits, and biosynthetic potential of selected bacterial endophytes. Based on strong *in vitro* antagonistic activity and frequent isolation, 15 representative strains were selected for whole-genome sequencing to uncover the genetic basis underlying their biocontrol potential. Genomes were sequenced using ONT long-read sequencing, enabling highly contiguous assemblies. Several genomes were resolved into single circularized contigs, while all assemblies exhibited high completeness (> 99%) and minimal contamination (< 1%) (Table S4), allowing reliable comparative and functional analyses, including accurate biosynthetic gene cluster (BGC) prediction. Genome sizes ranged from *c.* 4.4 Mb (*P. graminis*) to *c.* 6.0 Mb (*B. cereus*).

KEGG analysis revealed dominance of 'genetic information processing' and 'signaling/cellular processes' in all the strains except for *B. velezensis* 3–53, *B. subtilis* 9–155, and *B. pseudomycoides* 8–70 in which the main functions are 'carbohydrate metabolism', 'genetic information processing', and 'amino acid metabolism'. For the three *Pseudomonas* strains and the two *Erwinia* strains, the 'environmental information processing' category was dominant (Table S5).

At the protein level (OrthoVenn analysis), higher numbers of clusters were found in *B. cereus* 91–63, *B. mycoides* 8–62, and

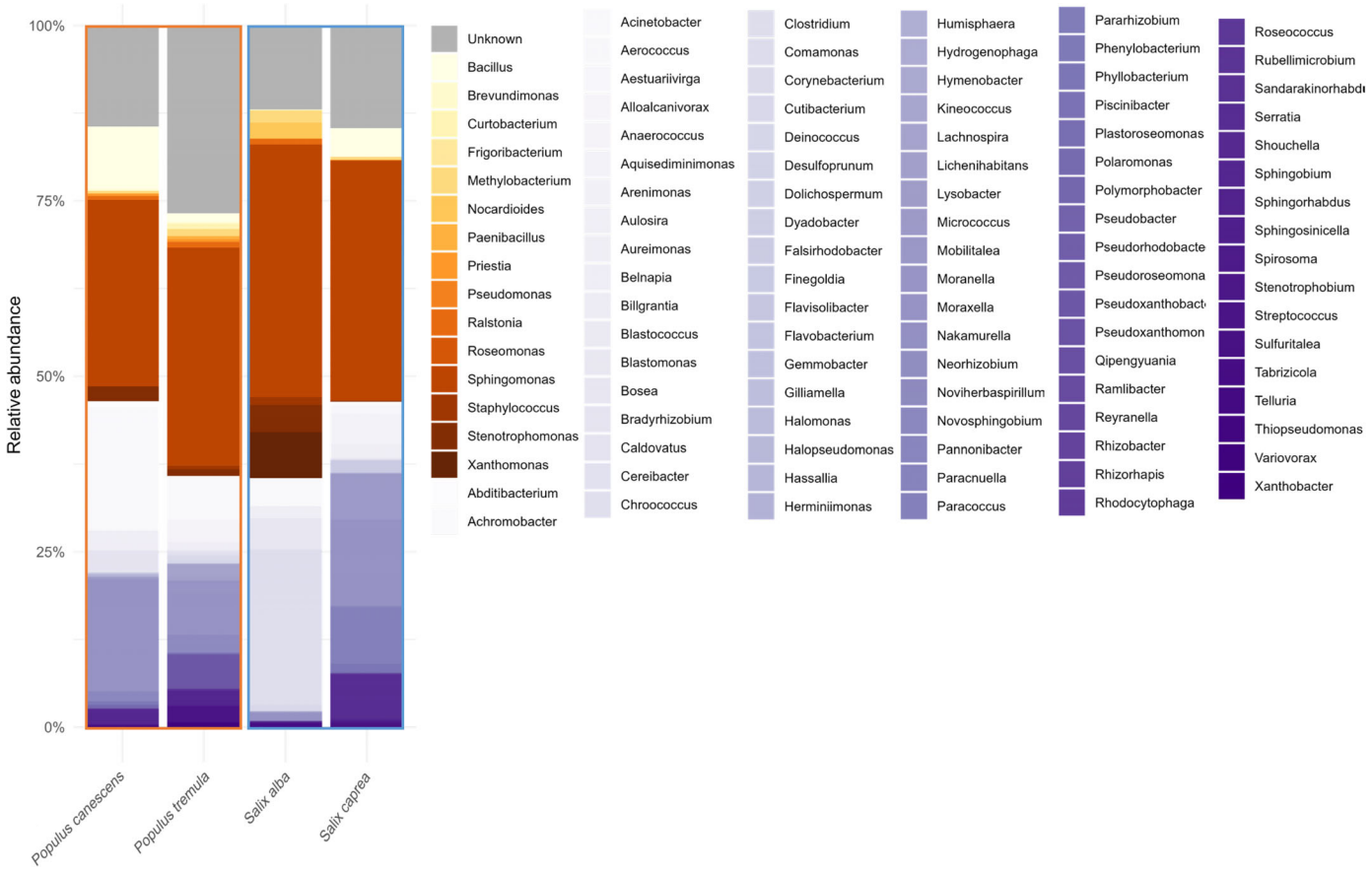

Fig. 2 Relative abundance of bacterial genera in *Salicaceae* species based on Illumina MiSeq 16S rRNA sequencing. Stacked barplots show genus-level composition for each plant species. Genera are colored by taxonomic groups. Poplar species display broader taxonomic diversity and evenness compared to willow, particularly in *Populus tremula*. Genera in shades of yellow-brown represent those also isolated via culturing, and therefore shared between culture-dependent and culture-independent approaches.

B. pseudomycoides 8–70 with 5038, 4966, and 4223 clusters, respectively (Fig. S7). These strains shared 1405 clusters of genes. The five *Bacillus* species shared 995 clusters genes, while the *Pseudomonas* strains 9–161 and 9–169 shared 1369. *Erwinia rhapontici* recorded the lowest number of gene clusters. Higher number of clusters (761) is shared between *Pseudomonas* and *Erwinia* strains. In total, 610 orthologous gene clusters were shared by all eight bacterial strains. All strains were able to inhibit *B. salicis*, *F. avenaceum*, and *F. culmorum* except *E. rhapontici* 11–25. When looking at clusters shared between all strains except *Erwinia*, we found 73 clusters genes comprising some gene clusters that may be implicated in direct antagonism such as 'protein secretion by the type II secretion system', 'response to antibiotic', and 'metallopeptidase activity' respectively.

Annotation of BGCs using antiSMASH identified diverse BGCs (Table S6). All *Bacillus* encoded bacillibactin, with subtilis-group strains also producing bacillaene, bacilysin, and surfactin; *B. velezensis* additionally carried difficidin, fengycin, and iturin. Other lineage-specific clusters included plipastatin and subtilosin (*B. subtilis*), paeninodin (*B. cereus* group), petrobactin (most strains), and kurstakin (*B. pseudomycoides/mycoides*). *Pseudomonas* encoded pyoverdine, phenazine, and aryl polyene, and *E. rhapontici* contained additional putative antagonistic BGCs.

Functional genome annotation using the VFDB database (Table S7) identified multiple virulence and defence-related traits, including type VI secretion systems, siderophore synthesis genes, and genes involved in adhesion, motility, and oxidative stress tolerance, particularly among *Pseudomonas* isolates. *Bacillus* strains encoded numerous immunity and stress response genes, as well as lipopeptide-associated biosynthetic loci.

PGPT-Pred analysis (Fig. S8) showed that plant colonization, biocontrol, and competitive exclusion dominated across strains. *Bacillus velezensis* and *Pseudomonas coleopterorum* were enriched in biocontrol functions, whereas *E. rhapontici* showed profiles biased toward colonization. Other PGPT categories occurred at lower abundance. Most strains shared core traits related to 'nutrient mobilization', 'stress tolerance', and 'pathogen suppression', consistent with bioinoculant potential.

PlaBase PIFAR profiles (Fig. S9) showed high toxin-related gene proportions in *B. velezensis*, *B. subtilis*, *Pseudomonas*, and *Erwinia*, indicating strong antagonistic potential. Exopolysaccharides, detoxification, and multidrug resistance genes were enriched in *Bacillus*, while hormone-related functions were similar across

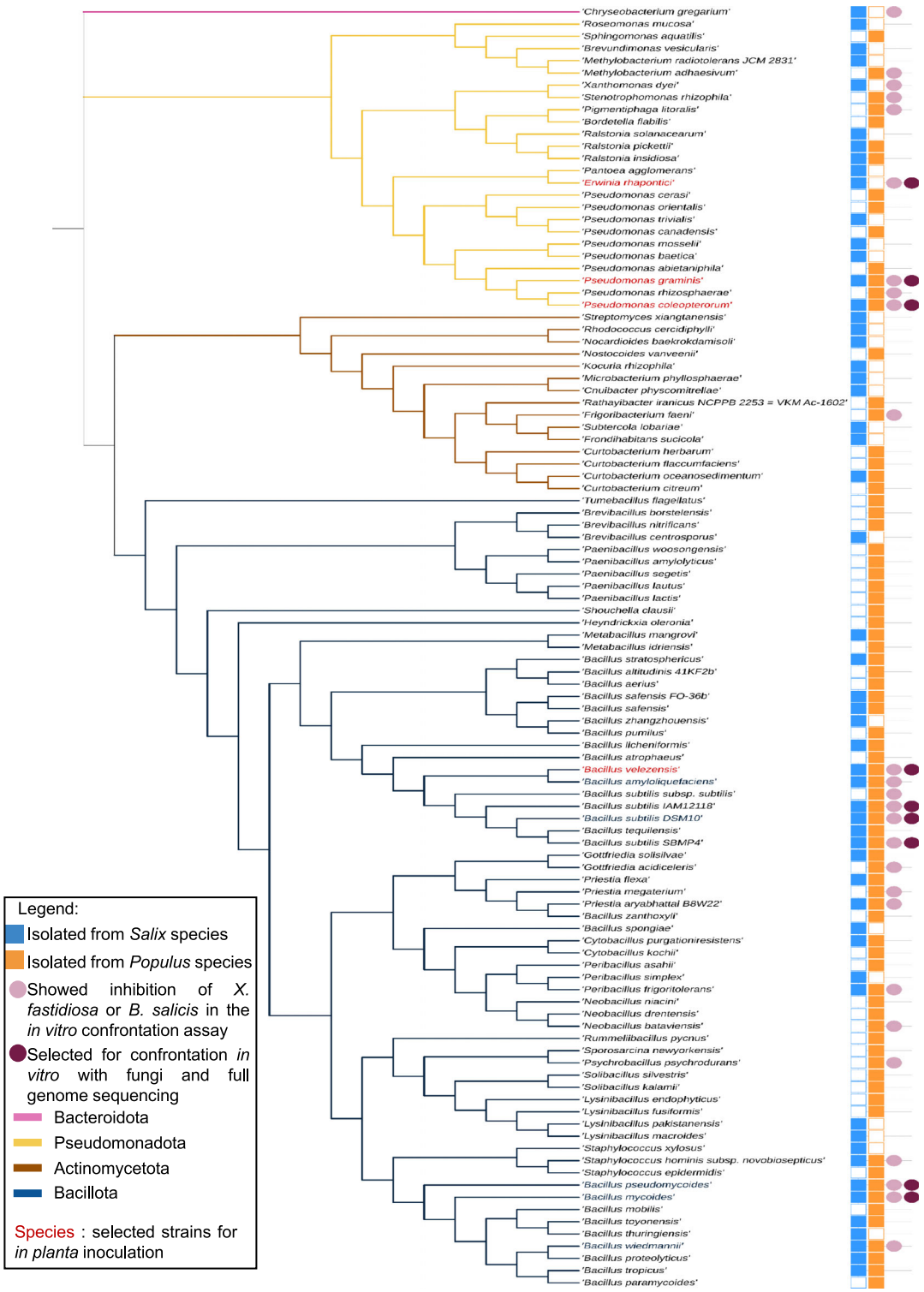

Fig. 3 Phylogenetic and functional overview of endophytic bacterial isolates exhibiting *in vitro* antagonism against *Brenneria salicis* and/or *Xylella fastidiosa*. A neighbor-joining phylogenetic tree was constructed from full-length 16S rRNA gene sequences. Branch colors correspond to the taxonomic affiliation of isolates at the phylum level: *Bacteroidota* (pink), *Pseudomonadota* (yellow), *Actinomycetota* (brown), and *Bacillota* (blue). Squares adjacent to isolate names indicate the plant host genus of origin: blue for *willow* and orange for *poplar*. Functional annotation indicating isolates that inhibited *B. salicis* and/or *X. fastidiosa* in confrontation assays (light purple circle), and strains selected for whole-genome sequencing and further characterization (dark purple circle). Strains used for the *in planta* inoculation are in red. This analysis highlights the phylogenetic diversity, host plant association, and functional potential of xylem-associated bacterial endophytes isolated from *Salicaceae* species.

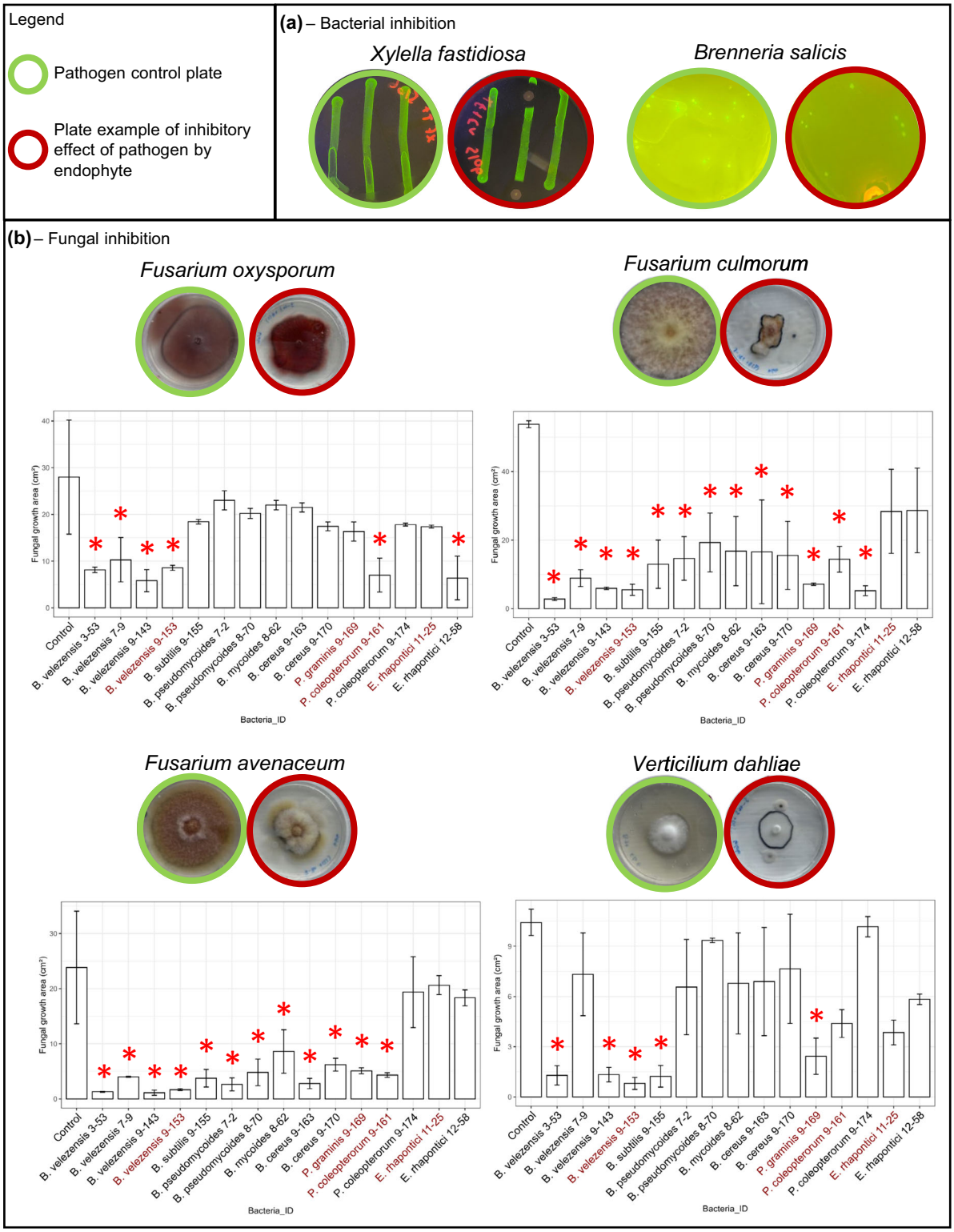

Fig. 4 Endophyte *in vitro* growth assay showing bacterial and fungal inhibition. (a) *In vitro* growth inhibition assays of *Xylella fastidiosa* and *Brenneria salicis*. Control treatments (green) are compared with representative Petri dishes cocultured with an endophytic bacterial isolate (red), illustrating the inhibitory effect. (b) Growth area in cm^2 of four vascular fungi (*Fusarium oxysporum*, *F. culmorum*, *F. avenaceum*, *Verticillium dahliae*) by 15 endophytic bacteria. Growth inhibition was measured 5 d after confrontation. A one-way ANOVA was conducted to assess the effect of 15 bacterial treatments on fungal growth for each fungal isolate. The analysis showed a significant treatment effect for all fungi (FA = 3.37, pA = 0.0019; FB = 2.77, pB = 0.0076; FC = 5.38, pC = 0.001; FD = 3.53, pD = 0.0013). Post hoc comparisons using Dunnett's test (Bonferroni-adjusted) indicated some treatments significantly reduced growth compared to the control. Stars above bars indicate fungi growth that are significantly lower as shown in the example Petri dish framed in red compared to the control measures in the Petri dish framed in green. Strains used for the *in planta* inoculation are in red.

strains. Competitive exclusion and niche-adaptation traits occurred at lower abundance. Overall, *Bacillus* displayed broader colonization and antagonism traits, whereas *Pseudomonas* and *Erwinia* relied more on toxin-associated functions (Table S8).

Generation and validation of fluorescently tagged strains for vascular tracking by PCR and qPCR

To enable the spatial monitoring of bacterial colonization within the xylem and to distinguish endophytic strains from vascular pathogens during co-inoculation assays, selected isolates were chromosomally tagged with distinct fluorescent markers. This strategy allowed the visualization of bacterial distribution patterns and the assessment of potential spatial overlap or segregation within the complex vascular environment. Transformation was successful for *B. salicis* LMG2698, *E. rhapontici* (11–25, 12–58), *Pseudomonas coleopterorum* 9–161, and *P. graminis* 9–169. Transconjugants of *B. salicis* and *E. rhapontici* were obtained via Tn*7*-based conjugation, and fluorescent colonies were selected on TSA with the appropriate antibiotic. Electroporation of *P. coleopterorum* and *P. graminis* with the Tn*7*-mCherry construct also yielded fluorescent transformants on spectinomycin LBA. Confocal microscopy confirmed fluorescence, and PCR with Tn7-specific primers verified site-specific integration of the mNeonGreen or mCherry cassette downstream of *glmS* (Fig. S10). Together, these fluorescent strains provided a robust toolset for tracking bacterial dynamics and evaluating potential colocalization patterns within host tissues.

In planta assay evaluating biocontrol potential of selected endophytic strains

To evaluate the ecological relevance and biocontrol potential of selected endophytic strains, a series of *in planta* assays was conducted using two host systems and two vascular pathogens. *N. tabacum* served as a model host to validate colonization dynamics and pathogen–endophyte interactions, whereas *S. caprea* was used as a representative *Salicaceae* woody host to assess ecological relevance within a lignified, perennial vascular system. Plants were inoculated with either *X. fastidiosa* or *B. salicis*, alone or in combination with selected endophytes, and monitored over one- and three-month experimental periods. Three parameters were assessed: (1) endophyte colonization and persistence in xylem tissues, (2) disease symptom mitigation, and (3) pathogen DNA loads. This design allowed discrimination between colonization ability and functional biocontrol activity across model and woody hosts. Two sampling points were used in all co-inoculation assays: T1, an intermediate sampling for qualitative PCR detection (2 wk in the 1-month assay; 1 month in the 3-month assay), and Tf, the final harvest (1 or 3 months), used for qPCR quantification, bacterial re-isolation, and confocal microscopy. These time points distinguished early colonization from long-term persistence and disease progression.

Tagged-endophytic bacteria inoculated in *N. tabacum* and *S. caprea* can colonize their xylem vessels Inoculation assay was performed with successfully transformed strains and one *B. velezensis* strain untransformed but part of the core-microbiome of tested *Salicaceae*.

To assess the ability of endophytic strains to establish *in planta*, bacterial presence was evaluated by PCR at T1 and Tf post inoculation, and by re-isolation from stem segments at Tf. In *N. tabacum*, all strains were detected by PCR at T1 in at least one plant, but none were detected at Tf. Nevertheless, successful re-isolation from 2 to 5 plants per strain confirmed bacterial persistence despite reduced PCR detectability. In *S. caprea*, similar trends were observed. No bacteria were detected in controls. These results indicate that all endophytes can colonize *N. tabacum* and *S. caprea* stems, with re-isolation confirming persistence despite transient PCR detection (Table S9; Fig. S11A,B).

Co-inoculation of tagged-endophytic and pathogenic bacteria showed a mitigation of symptoms in *N. tabacum* and *S. caprea* *Tobacco plants.* In the one-month assay, symptoms in *X. fastidiosa*-only plants were more pronounced than in co-inoculated plants (Fig. 5a). But, no significant difference in plant height was detected across treatments (Fig. S12A). qPCR analysis revealed a significant effect of treatment on Cq pathogen values (ANOVA, $F = 10.31$, $P = 7.19e\text{-}11$). Plants inoculated with *X. fastidiosa* alone showed significantly lower Cq values than plants co-inoculated with any endophyte (Tukey's HSD, $P < 0.05$). For *B. salicis*, the pathogen-only treatment showed significantly lower Cq values than co-inoculations with *B. velezensis* and *P. coleopterorum* (Tukey's HSD, $P < 0.05$), whereas no significant differences were detected with the other endophytic strains: *E. rhapontici*, *P. graminis*, and *P. phytofirmans* (Tukey HSD, $P > 0.05$; Fig. 5b). qPCR endophyte quantification revealed variable persistence across treatments (Fig. S12B; Table S10).

However, in the three-month assay, visual symptom scoring over the experimental period revealed clear differences between treatments. Plants inoculated with *X. fastidiosa* or *B. salicis* alone developed the most severe symptoms, including wilting and stunting. By contrast, co-inoculation with certain endophytes, notably *E. rhapontici* and *P. phytofirmans*, visibly reduced symptom severity compared with pathogen-only controls. Endophyte-only treatments and mock controls exhibited minimal to no symptoms (Fig. 5c). These observations were consistent with significant differences in final plant height (ANOVA, $F = 7.475$, $P = 6.72E\text{-}10$): In both *X. fastidiosa*– and *B. salicis*–inoculated plants, co-inoculated treatments generally produced taller plants than pathogen-only controls, with several pairwise comparisons being statistically significant (Tukey's HSD, $P < 0.05$; Fig. 5e). Isolation assays confirmed the presence of pathogens and/or endophytes in a subset of plants (Fig. S13A), with co-inoculated treatments generally showing fewer successful pathogen re-isolations compared with pathogen-only controls. Confocal microscopy detection (Figs 6, S13B) confirmed the presence of fluorescently labeled endophytes and pathogens in vascular tissues for some treatments. qPCR-based pathogen quantification revealed a significant effect of the inoculation treatment on *X. fastidiosa* Cq values (ANOVA, $F = 29.33$, $P = 1{,}14e\text{-}03$). Plants co-inoculated with *E. rhapontici*, *P. coleopterorum*, or *P. graminis*

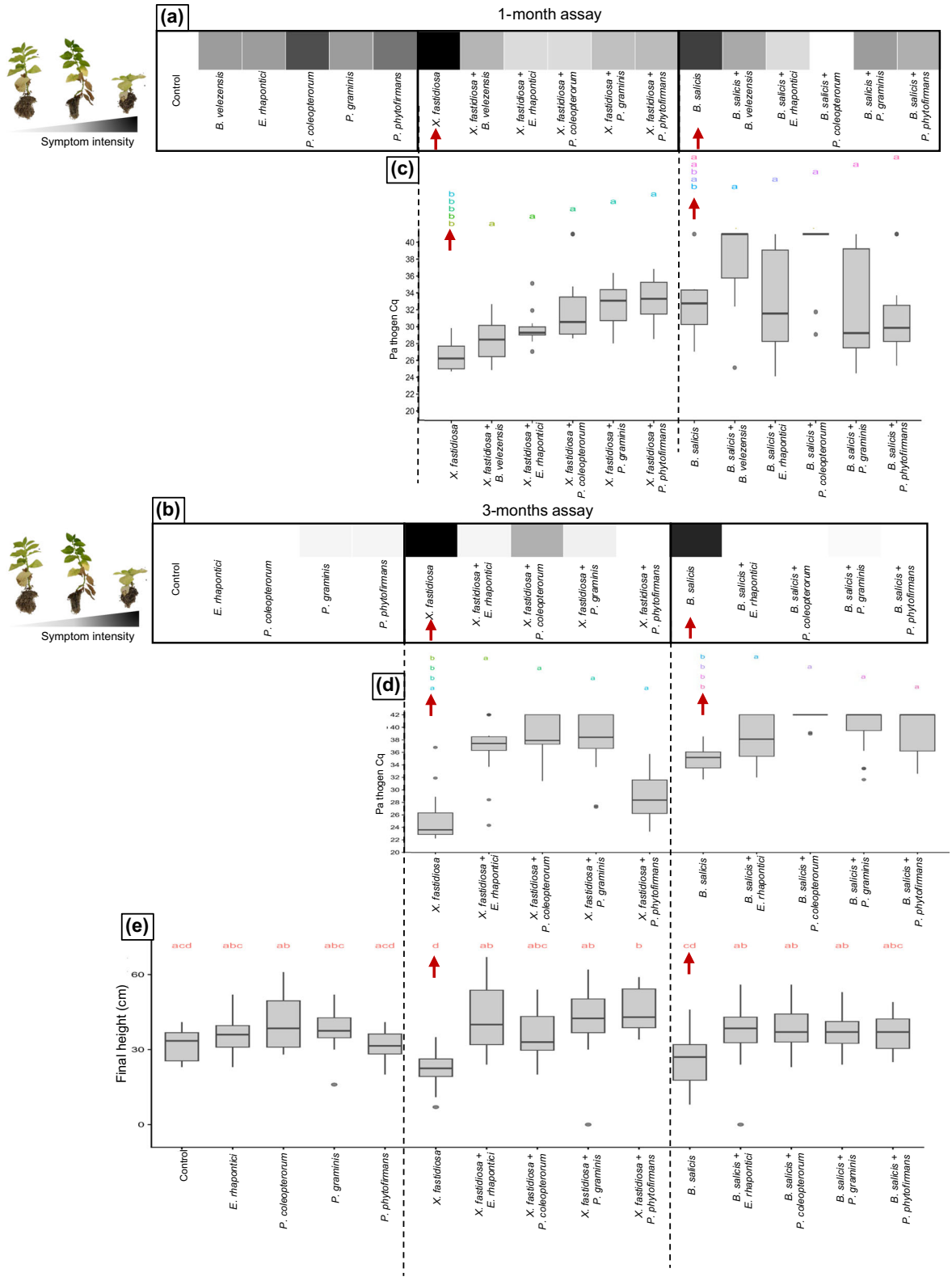

exhibited significantly higher Cq values than plants inoculated with *X. fastidiosa* alone (Tukey's HSD, $P < 0.05$), whereas no significant difference was observed with *P. phytofirmans*. For *B. salicis*, the pathogen-only treatment showed significantly lower Cq values than co-inoculations with any endophyte (Tukey's HSD, $P < 0.05$; Fig. 5d). qPCR endophyte quantification

Fig. 5 Symptoms, growth, and pathogen load in the *in planta* assay on *Nicotiana tabacum*. Visual scale to monitor symptom development on tobacco plants during the one-month assay (a) and three-month assay (b), ranging from asymptomatic (white) plants to severely wilted and stunted individuals (black) and heatmap displaying the average severity of symptoms for each treatment group. The darker shades indicate stronger symptom expression. Red arrows show more symptomatic plants when inoculated with pathogen alone. (c) Cq values obtained from quantitative polymerase chain reaction (qPCR) for each treatment group, where lower Cq values indicate higher pathogen DNA quantity. Treatments are grouped according to the inoculated pathogen (*Xylella fastidiosa*, left of the dashed line; *Brenneria salicis*, right). Colored letters above boxplots denote statistical groupings based on Tukey's HSD *post hoc* tests ($P < 0.05$), comparing each pathogen-only treatment with its corresponding pathogen + endophyte co-inoculations. Identical letters indicate no significant difference, whereas distinct letters identify significant pairwise differences. (d) Cq values obtained from qPCR for each treatment group, in which lower Cq values indicate higher pathogen DNA quantity. Treatments are grouped according to the inoculated pathogen (*X. fastidiosa*, left of the dashed line; *B. salicis*, right). Colored letters above boxplots denote statistical groupings based on Tukey's HSD *post hoc* tests ($P < 0.05$), comparing each pathogen-only treatment with its corresponding pathogen + endophyte co-inoculations. Identical letters indicate no significant difference, whereas distinct letters identify significant pairwise differences. (e) Final height (in cm) of tobacco plants at harvest. Different letters indicate significant differences between treatments within block (=pathogen group) and pathosystems (=pathogen + endophyte group) (Tukey's HSD test, $P < 0.05$).

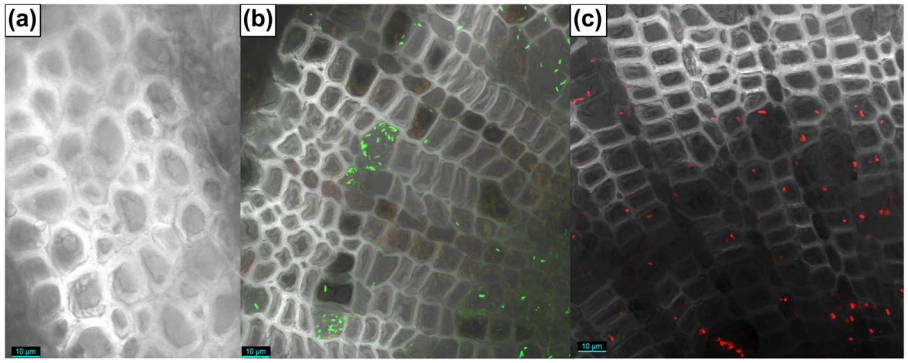

Fig. 6 Transversal section of *Salix caprea* inoculated with *Xylella fastidiosa* and *Erwinia rhapontici*. Confocal microscopy was used to see presence and distribution of inoculated bacteria. (a) *X. fastidiosa* was often observed as single cells attached to the vessel wall. (b) *E. rhapontici* was also detected in some vessels but never colocalized in the same section than the pathogen. Supplementary images of inoculated plant samples can be found in Supporting Information Fig. S18. Bars, 10 μm.

revealed variable persistence across treatments. In *X. fastidiosa* infections, *E. rhapontici* and *P. phytofirmans* reached detectable levels in some plants, whereas *P. graminis* and *P. coleopterorum* persisted at low level. Other trends were observed in *B. salicis* infections with no detection of *P. phytofirmans* and low loads of others (Fig. S14; Table S10).

Willow plantlets. Across two co-inoculation assays involving *X. fastidiosa* or *B. salicis* and selected endophytic strains in willow *in vitro* plantlets, contrasting responses in plant growth, pathogen load, and detection rates were recorded. The one-month assay included *B. velezensis* 9–153, while the three-month assay excluded this strain.

In the one-month assay, symptoms in *B. salicis*-only plants were more pronounced than in co-inoculated plants (Fig. 7a). But no significant difference in plant height was detected across treatments (Fig. S15A). No significant differences in pathogen Cq value were detected neither in *X. fastidiosa*-inoculated plants nor in *B. salicis-inoculated* plants ($F = 19.35$, $P > 0.05$; Fig. 7b). qPCR endophyte quantification revealed variable persistence across treatments (Fig. S15B; Table S10).

In the three-month assay, symptoms in *pathogen*-only plants were more pronounced than in co-inoculated plants (Fig. 7c). However, qPCR pathogen quantification analysis showed no significant differences among treatments ($F = 7.499$, $P > 0.05$; Fig. 7d). qPCR detection of endophyte DNA revealed persistence and no significant difference across treatments ($F = 1.94$, $P > 0.05$; Fig. S16; Table S10). Isolation assays confirmed the presence of the inoculated bacteria in a subset of plants (Fig. S17A), with pathogen recovery rates generally quite low. Confocal microscopy detection (Figs 6, S17B) verified the colonization of vascular tissues by fluorescently labeled endophytes and pathogens in some treatments. No significant differences in final height were detected among *X. fastidiosa* and *B. salicis* treatments (Fig. 7e).

Discussion

This study aimed at defining the bacterial microbiome of the xylem sap from *Salicaceae* species, using an integrated framework combining culture-dependent and culture-independent approaches, functional *in vitro* assays, and genome mining of selected isolates. Beyond descriptive characterization, our multiphasic strategy was designed to identify endophytic bacteria that are ecologically adapted to the highly specialized xylem environment, an oligotrophic, pressurized niche in which many conventional biocontrol agents fail to establish and persist. The results show both the complementarity of culture-dependent and -independent approaches, and highlight the functional and genomic potential of endophytic strains for biocontrol applications. Over 400 bacteria from 43 genera and 104 species were isolated from xylem sap. Metabarcoding sequencing uncovered 158 genera from 13 phyla. Several strains (e.g. *B. velezensis*, *P. coleopterorum*) showed dual antagonism against pathogenic bacteria and fungi. Genomic mining revealed diverse BGCs, low virulence potential, and traits associated with biofilm formation, and a low virulence potential. By linking ecological prevalence, functional antagonism, and genomic traits potentially related to vascular

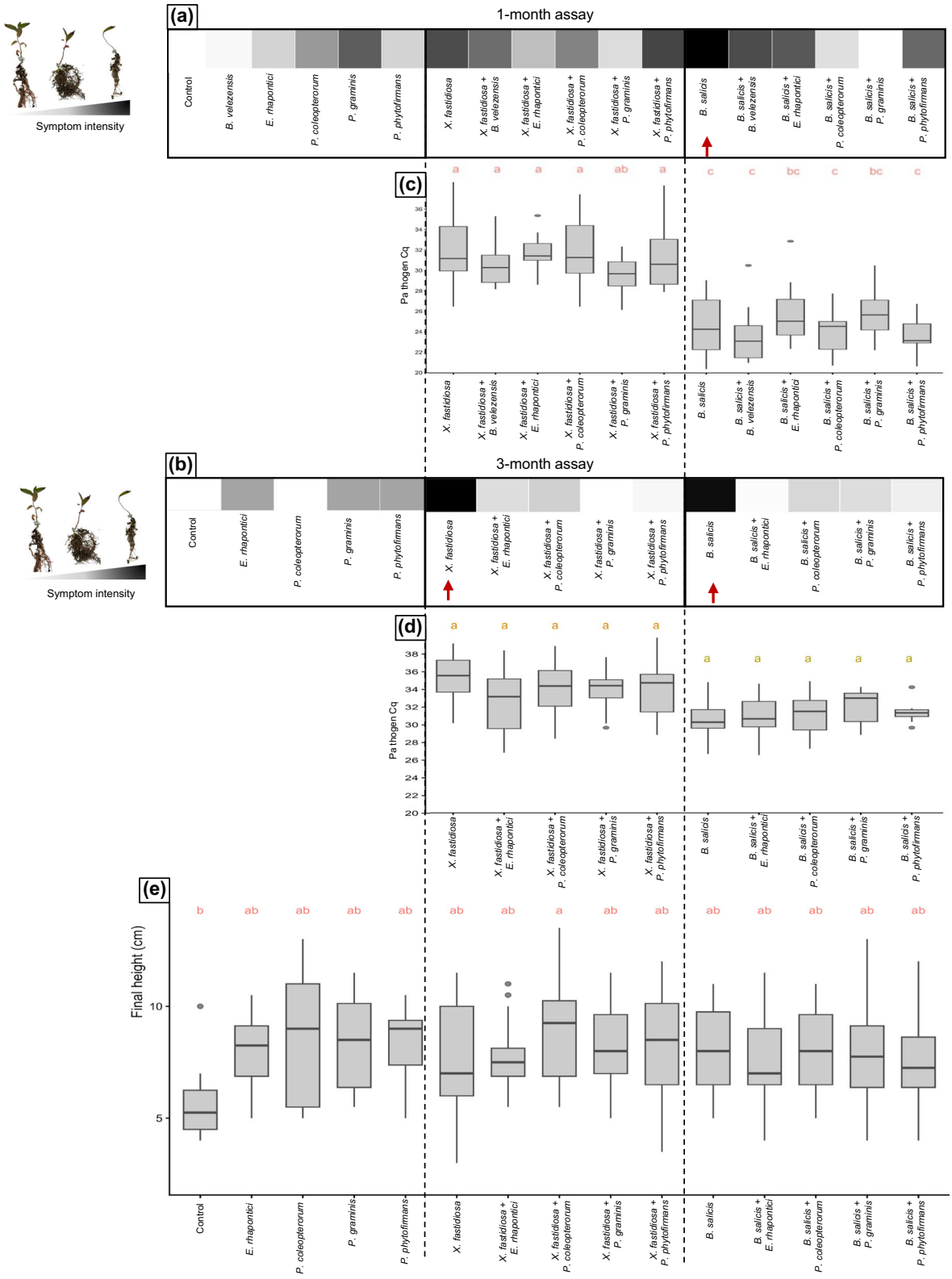

fitness and persistence, our approach moves beyond inventorying diversity and instead establishes a rational framework for selecting 'specialized xylem allies' against pathogenic bacteria such as *X. fastidiosa* or *B. salicis*. This initial characterization of the *Salicaceae* xylem bacterial microbiome constitutes a foundational step toward developing a promising strategy for identifying candidate

Fig. 7 Symptoms, growth and pathogen load in the *in planta* assay on *Salix caprea*. Visual scale to monitor symptom development on willow *in vitro* plantlets during the one-month assay (a) and 3-month assay (c), ranging from asymptomatic (white) plants to severely wilted and stunted individuals (black) and heatmap displaying the average severity of symptoms for each treatment group. Darker shades indicate stronger symptom expression. Red arrows show more symptomatic plants when inoculated with pathogen alone. (b) Cq values obtained from quantitative polymerase chain reaction (qPCR) for each treatment group, in which lower Cq values indicate higher pathogen DNA quantity. Treatments are grouped according to the inoculated pathogen (*Xylella fastidiosa*, left of the dashed line; *Brenneria salicis*, right). Colored letters above boxplots denote statistical groupings based on Tukey's HSD *post hoc* tests ($P < 0.05$), comparing each pathogen-only treatment with its corresponding pathogen + endophyte co-inoculations. Identical letters indicate no significant difference, whereas distinct letters identify significant pairwise differences. (d) Cq values obtained from qPCR for each treatment group, in which lower Cq values indicate higher pathogen DNA quantity. Treatments are grouped according to the inoculated pathogen (*X. fastidiosa*, left of the dashed line; *B. salicis*, right). Colored letters above boxplots denote statistical groupings based on Tukey's HSD *post hoc* tests ($P < 0.05$), comparing each pathogen-only treatment with its corresponding pathogen + endophyte co-inoculations. Identical letters indicate no significant difference, whereas distinct letters identify significant pairwise differences. (e) Final height (in cm) of willow *in vitro* plantlets at harvest. Different letters indicate significant differences between treatments within bloc (= pathogen group) and pathosystems (=pathogen + endophyte group) (Tukey's HSD test, $P < 0.05$).

biological control agents that are ecologically adapted to the specific niche in which they may be deployed.

Host plant species and culture media influence the xylem-microbiota and shape recovery profiles

Composition and diversity of xylem-associated bacterial communities were significantly influenced by host plant species, with *P. canescens* exhibiting the highest richness and diversity across both culture-dependent and independent datasets. This aligns with earlier reports suggesting host-dependent structuring of poplar endophytes. Firrincieli *et al.* (2020) and Cheng *et al.* (2023) showed that microbiome composition varies with host genotype and environment. Such patterns support the hypothesis that host traits (e.g. xylem anatomy, sap chemistry, or immune signaling) filter microbial colonizers. Poplar endophytes also carry horizontally acquired genes (Taghavi *et al.*, 2005) and exhibit biocontrol activity (Doty *et al.*, 2023), suggesting an adaptive recruitment of functionally beneficial taxa. The higher functional diversity observed in *P. canescens* supports this host-driven assembly concept. By contrast, willow species generally supported less diverse and more *Bacillus*-dominated culturable communities, possibly due to narrower xylem ecological niches or differences in cavitation resistance, which could affect microbial colonization dynamics (Cochard *et al.*, 2007). Interestingly, Allsup *et al.* (2023) demonstrated that shifts in tree-associated microbial communities can enhance tolerance to environmental stressors in poplar, reinforcing the idea that microbiome flexibility may vary between *Salicaceae* genera.

Our results also highlight the importance of using multiple culture media for bacterial recovery (Compant *et al.*, 2005b; Hardoim *et al.*, 2015; Doty *et al.*, 2023). Because plates were monitored for only 3 d, slow-growing taxa may have been underrepresented, likely leading to an underestimation of total culturable diversity. Both host identity and culture conditions act as strong determinants of the xylem microbiome composition in *Salicaceae*, and support the idea that poplar species may offer broader ecological niches for microbial colonization and functional recruitment.

Culturable xylem-associated bacteria ranged from 8 & 10^1 to 6 & 10^2 CFU ml^{-1}, depending on the *Salicaceae* species and medium, in accordance with ranges measured for other woody crops (Gardner *et al.*, 1982; Bell *et al.*, 1995; Anguita-Maeso *et al.*, 2020).

Complementarity of culture-dependent and -independent approaches & identification of key taxa

Culture-dependent and -independent methods differed in microbial diversity with metabarcoding identifying 158 genera and 223 species, vs 43 genera and 104 species in culture. Shared dominant taxa indicate a core culturable fraction of the endophytic microbiota consistent with studies showing that a few dominant, culturable xylem endophyte genera play a disproportionate functional role in woody plants (Compant *et al.*, 2005b; Hardoim *et al.*, 2015; Deyett & Rolshausen, 2020; Zicca *et al.*, 2020). Some dominant cultured taxa were also detected by sequencing but at lower relative abundance, reflecting their overrepresentation in culture-based approaches. By contrast, several taxa abundant in amplicon data were not recovered in culture, consistent with their fastidious growth requirements. While *Bacillus*-dominated culture-dependent datasets across all tree species, amplicon sequencing revealed Pseudomonadota as the most abundant phylum, a pattern frequently reported when comparing cultivation and molecular surveys (Thomas & Shaik, 2020; Faddetta *et al.*, 2021). The low recovery of Pseudomonadota in culture indicates that much of the xylem microbiome is cultivation-recalcitrant, likely adapted to the oligotrophic and pressurized xylem environment poorly reproduced *in vitro* (Hardoim *et al.*, 2015). These taxa may rely on host metabolites or microbial interactions, meaning the culturable fraction captures only part of the functional diversity and is biased toward fast-growing species. This hidden diversity may include traits important for vascular stability, pathogen exclusion, or host adaptation (Thomas & Shaik, 2020; Faddetta *et al.*, 2021).

Together, these findings emphasize the complementarity of both approaches: while culture-dependent methods allow for downstream functional and genomic studies, culture-independent sequencing provides a more comprehensive overview of the xylem microbiome structure (Table 2). Integrating both approaches remains essential for understanding and exploiting plant-associated microbiomes, particularly in perennial crops (Anguita-Maeso *et al.*, 2020; Lengrand *et al.*, 2025).

Table 2 Comparison between culture-dependent and culture-independent approaches for profiling xylem-associated bacterial communities in *Salicaceae* species.

Aspect	Culture-dependent approach	Culture-independent approach
Method	Bacterial isolation on four agar media (BCYE, TSA, KB, PDA)	16S rRNA amplicon sequencing (V1V3 and V3V4 regions)
No. of samples analyzed	6 replicates per species × 6 species at 2 different time point	6 replicates per species × 4 species
Total OTUs/ genera identified	43 genera, 104 species, 4 phyla	158 genera, 223 species, 13 phyla
Dominant phyla	*Bacillota*, *Pseudomonadota*	*Pseudomonadota*, *Bacillota*, *Actinomycetota*
Core taxa	*Bacillus*, *Priestia*, *Pseudomonas*	*Pseudomonas*, *Sphingomonas*, *Ralstonia*
Unique taxa recovered	Cultivable, fast-growing, spore-formers	Could include unculturable, fastidious, low-abundance taxa
Bias/Limitations	Strong selectivity of media; underestimates diversity	Sensitive to primer bias and DNA extraction efficiency
Strengths	Enables strain isolation for functional assays	Provides comprehensive overview of microbiome composition
Complementarity	Provides live isolates for downstream use	Broadens taxonomic resolution and reveals rare taxa

Functional screening and genome mining reveal promising biocontrol candidates

Increasing evidence supports the beneficial impact of endophytic bacteria on their host plants, particularly through indirect mechanisms such as pathogen inhibition (Santoyo *et al.*, 2016; Afzal *et al.*, 2019). This positions endophytic bacteria as promising candidates for biocontrol, given their potential to outcompete pathogens within shared ecological niches. In our study, 15 endophytic bacterial strains demonstrated clear *in vitro* antagonistic activity against various xylem-associated pathogens.

Interestingly, these species have previously been reported across a wide range of plant hosts and microenvironments except *E. rhapontici* not currently used as a biocontrol agent; on the contrary, it is known to be a plant pathogen associated with diseases (Walsh *et al.*, 2001; Huang *et al.*, 2003, 2005; Mikiciński *et al.*, 2016; Collazo *et al.*, 2017; Wu *et al.*, 2020; Di *et al.*, 2023; Elsharawy *et al.*, 2023; Sorokan *et al.*, 2023; Alattas *et al.*, 2024; Das *et al.*, 2024; Shahzad *et al.*, 2024; Wang *et al.*, 2024, 2025; Zhong *et al.*, 2024). Nevertheless, it was recovered here from the *Salicaceae* endosphere, highlighting the importance of selecting BCAs able to colonize xylem tissues targeted by pathogens such as *X. fastidiosa*, *B. salicis*, *F. oxysporum*, *F. culmorum*, *F. avenaceum*, and *V. dahliae*.

In vitro antagonism may result from mechanisms such as lytic enzyme, space and/or nutrients competition (Poppe *et al.*, 2003; Compant *et al.*, 2005a; Zicca *et al.*, 2020). Moreover, secondary metabolite production in dual *in vitro* assays depends on the nutrient concentration and composition of the growth medium. However, confrontation assays can be difficult to interpret, especially with slow-growing pathogens such as *X. fastidiosa*, where apparent inhibition may reflect nutrient depletion rather than true antagonism (Köhl *et al.*, 2019; Mourou *et al.*, 2022). Only strains showing clear and reproducible inhibition were therefore retained. Functional activity does not guarantee suitability as a biocontrol agent. Some taxa, including *E. rhapontici* and the *Bacillus cereus* group, contain pathogenic strains, but the isolates tested showed no symptoms and few virulence genes (Table S7). Strain-level evaluation is required; some isolates are better suited as ecological models, whereas *B. velezensis* and selected *Pseudomonas* spp. are more promising candidates, pending further safety assessment. Genomic analysis of the 15 isolates revealed diverse traits linked to plant growth promotion and antagonism, with core metabolic functions predominating (Taghavi *et al.*, 2010; Martínez-Hidalgo *et al.*, 2015; Slama *et al.*, 2019; Nicotra *et al.*, 2024). Shared clusters included type II secretion, metallopeptidases, and antibiotic-response genes, associated with enzyme delivery and microbial competition (Tilley *et al.*, 2014; Urusova *et al.*, 2019; Rigo *et al.*, 2023). Predicted functions related to colonization, stress tolerance, and competitive exclusion were common across strains, consistent with previous studies on beneficial endophytes (Pieterse *et al.*, 2014; Patz *et al.*, 2021). *Bacillus velezensis* strains showed particularly strong enrichment in biocontrol-related genes, in line with their antifungal activity and with the well-established antimicrobial potential of the *B. subtilis* species complex, driven largely by NRPS- and PKS-encoded metabolites such as surfactin and fengycin (Ongena *et al.*, 2007; Rabbee *et al.*, 2023). By contrast, members of the *B. cereus* group harbored a more restricted set of BGC, consistent with previous reports. Differences in biosynthetic potential among *Bacillus* strains may partly explain their contrasting antagonistic spectra. For instance, the absence of bacillothiazol and plantazolicin in the only *B. velezensis* strain lacking activity against *V. dahliae* suggests a possible role for these metabolites in antifungal activity, although functional validation is required (Hasan *et al.*, 2020; Shen *et al.*, 2022; Wang *et al.*, 2022). Likewise, the exclusive presence of kurstakin in *B. pseudomycoides* and *B. mycoides* may contribute to their broader inhibitory capacity. The strong biocontrol performance of *Pseudomonas* strains is consistent with their predicted genomic repertoire, notably the presence of BGCs encoding pyoverdine, phenazines, and aryl polyenes. These metabolites are commonly associated with iron acquisition, oxidative stress protection, and antifungal activity, and likely contribute to the inhibitory phenotypes observed *in vitro*. More broadly, species within the genus *Pseudomonas* are well-documented ecological competitiveness and production of diverse antimicrobial compounds, including cyclic lipopeptides, phenazines, hydrogen cyanide, and pyrrolnitrin (Haas & Défago, 2005; Loper *et al.*, 2012; Raaijmakers & Mazzola, 2012). Although such compounds were not specifically predicted in the genomes analyzed here, their widespread occurrence within the genus underscores the established biocontrol capacity of *Pseudomonas* spp. and

provides ecological context and proof of their efficacy against multiple plant pathogens are well-established (Zhang *et al.*, 2015; Anzalone *et al.*, 2021; Felipe *et al.*, 2021). Overall, our results confirm the central role of *Bacillus* and *Pseudomonas* as dual-function PGP and biocontrol agents, which underpins their dominance in commercial bioinoculants (Backer *et al.*, 2018). Importantly, however, strains from less explored genera such as *Erwinia* also displayed clear PGP and antagonistic potential, highlighting *Salicaceae* endophytes as a valuable and still under-exploited reservoir of beneficial microbes.

In planta effect of co-inoculation

Growing evidence shows that bacterial endophytes contribute to plant growth and health, notably through indirect mechanisms such as pathogen suppression and plant growth simulation (Afzal *et al.*, 2019; Santoyo, 2022), positioning them as promising BCAs able to compete with xylem-limited pathogens such as *X. fastidiosa* (Lacava *et al.*, 2007; Azevedo *et al.*, 2016; Zicca *et al.*, 2020) or *B. salicis*. Standard biocontrol agents often fail in woody hosts due to lack of fitness in the oligotrophic and high-pressure xylem environment. Our approach integrates ecological prevalence, functional antagonism, and genomic traits linked to persistence. This pipeline provides a rational framework for selecting 'specialized xylem allies' suitable for vascular delivery strategies.

All tested endophytes were detectable within xylem tissues at early time points, as confirmed by microscopy, re-isolation, and qPCR, although at low concentration, indicating limited persistence or heterogeneous vascular distribution. Detection frequencies declined at Tf in several single-inoculation treatments, suggesting that long-term persistence was variable among strains. Nondetection at Tf may reflect a reduction in bacterial populations below the assay detection threshold, spatially restricted colonization not captured in sampled tissues, competitive displacement over time, or effective clearance by host responses. These observations suggest that, for some strains, early or transient establishment within the xylem may be sufficient to influence pathogen dynamics and disease development, even in the absence of stable high-density persistence. However, co-inoculation consistently mitigated disease symptoms in tobacco in which pathogen-only plants exhibited the most severe wilting and growth reduction (Fig. 5a,b). Co-inoculation treatments enhanced plant growth at 3 months (Fig. 5e). This protective effect was associated with reduced pathogen loads in tobacco, with *X. fastidiosa* significantly decreased in all co-inoculated treatments during the one-month assay (Fig. 5c) and remaining reduced at 3 months except when co-inoculated with *P. phytofirmans* (Fig. 5d). By contrast, *B. salicis* loads were reduced only in co-inoculations with *B. velezensis* or *P. coleopterorum* at one month (Fig. 5c), but were significantly lower across all co-inoculated treatments at 3 months compared with pathogen-only controls (Fig. 5d). In *S. caprea* plantlets, co-inoculation with endophytic bacteria was associated with a visible attenuation of disease symptoms compared with pathogen-only treatments (Fig. 7a,b), together with a tendency toward enhanced plant height (Fig. 7e), but neither the one-month nor the three-month assays revealed significant differences in *X. fastidiosa* or *B. salicis* loads among treatments (Fig. 7c,d). One plausible explanation is interference with pathogen biofilm formation and vascular occlusion rather than outright population suppression, as biofilm development is a key virulence determinant of *X. fastidiosa*, driving vessel clogging and hydraulic dysfunction (Marques *et al.*, 2002; Chatterjee *et al.*, 2008; Cruz *et al.*, 2012). Endophytic bacteria can disrupt these processes, as illustrated for *Methylobacterium extorquens*, which co-colonizes xylem vessels with *X. fastidiosa* and reduces biofilm formation while altering pathogen spatial organization but without eliminating the pathogen, and for other xylem endophytes that limit pathogen accumulation and virulence through effects on quorum sensing, nutrient availability, or surface attachment (Filho *et al.*, 2012; Azevedo *et al.*, 2016). In this context, the low and heterogeneous bacterial loads detected by qPCR may reflect spatially restricted interactions with disproportionate functional consequences for disease development, as the spatial co-occurrence of pathogen- and damage-associated molecular patterns (Pathogen Associated Molecular Patterns (PAMPs) and Damage Associated Molecular Patterns (DAMPs)) can trigger strong, localized immune responses in plant tissues (Lindow *et al.*, 2024). Such spatial coincidence has been shown to amplify defence activation in root cells, highlighting the importance of fine-scale microbial localization in shaping host immune outcomes (Zhou *et al.*, 2020). Additionally, the low loads of *X. fastidiosa* detected in *S. caprea* likely explain the absence of similar effects as those shown on tobacco, consistently with previous findings on *X. fastidiosa* inoculation in *S. caprea* (Casarin *et al.*, 2022). The generally low detection and recovery of *B. salicis* further indicate reduced establishment under our experimental conditions. Although both pathogens have previously been reported on *S. caprea* (Turner *et al.*, 1992; Casarin *et al.*, 2022), our results suggest that this species might be more resistant than previously thought, highlighting the need for further studies with other *Salix* or *Populus* species. Together, these results highlight the strong but host-dependent biocontrol potential of *Salicaceae*-associated endophytes and suggest that their effect may rely on indirect mechanisms such as modulation of host defence responses or interference with symptom development rather than solely through pathogen suppression.

These results are consistent with previous reports showing that endophytic bacteria can antagonize vascular pathogens through multiple mechanisms, including niche competition, antibiosis, or induction of host defence responses (Compant *et al.*, 2005a, 2005b; Hardoim *et al.*, 2015). For instance, *Methylobacterium* and *Curtobacterium* species can limit *X. fastidiosa* colonization in grapevine and citrus (Araújo *et al.*, 2002; Lacava *et al.*, 2004, 2007; Azevedo *et al.*, 2016), while *P. phytofirmans* PsJN, a highly fit xylem endophyte in grapevine, promotes plant growth and tolerance to biotic stress and reaches high xylem populations ($> 10^6$CFU g plant^{-1}, Baccari *et al.*, 2019; Bragard *et al.*, 2019a, 2019b). Such high endophytic fitness and extensive xylem colonization appear critical for effective suppression of *X. fastidiosa*, a condition that was only partially met by tobacco- and willow-

associated endophytes in our system. However, our results indicate that measurable protective effects can also arise from early or spatially localized interactions, even when long-term persistence is limited. Accordingly, the limited pathogen loads and lack of clear effects on *B. salicis* may reflect restricted vascular movement, active host defences, or competition for xylem niches, underscoring the importance of host genotype and environmental context in shaping colonization outcomes. Beyond *in planta* interactions, an emerging frontier concerns the ecological persistence and dissemination of beneficial endophytes, including their ability to survive in xylem-feeding insect vectors, as shown for *Methylobacterium* spp. persisting in insect foreguts and interfering with *X. fastidiosa* transmission or biofilm formation (Gai *et al.*, 2009).

Here, particular attention should be given to the findings obtained for *B. salicis*. While microbiome-based biocontrol strategies have increasingly been investigated for *X. fastidiosa*, the potential of leveraging native xylem endophytes to mitigate watermark disease has remained largely unexplored. To date, *B. salicis* has primarily been studied from a pathogenicity and epidemiological perspective, with limited attention to microbial interactions within the xylem niche. The present study therefore fills an important knowledge gap by demonstrating that members of the resident xylem microbiome attenuate symptom development and may reduce pathogen loads.

Together, our results highlight the capacity of resident xylem endophytes to influence vascular pathogen dynamics and disease outcomes, providing a foundation for the future development of endotherapy approaches in woody hosts.

Acknowledgements

The research was supported by the National Fund for Scientific Research (FNRS) and the Université catholique de Louvain (UCLouvain). LP was a fellow at the Foundation for Training in Industrial and Agricultural Research (FRIA, FNRS). This research was also supported by the EFSA grant GP/EFSA/PLANTS/2022/04.

Competing interests

None declared.

Author contributions

LP and CB designed the study and drafted the manuscript. LP collected the data, performed the analyses, collected and interpreted the results. AK, SL, FM and CF contributed to the study (experimentations and data analysis). SR and FD provided material. All authors read and approved the final manuscript.

ORCID

Claude Bragard https://orcid.org/0000-0003-3169-1716
Frédéric Debode https://orcid.org/0009-0007-7525-0417
Alexandra Kahn https://orcid.org/0000-0001-6308-238X
Salomé Lengrand https://orcid.org/0009-0003-0914-7981
Lena Pesenti https://orcid.org/0000-0002-6829-395X

Data availability

Individual fastq files have been deposited in the Sequence Read Archive (SRA) database at the NCBI under BioProject accession no. PRJNA1377930.

References

Afzal I, Shinwari ZK, Sikandar S, Shahzad S. 2019. Plant beneficial endophytic bacteria: Mechanisms, diversity, host range and genetic determinants. *Microbiological Research* **221**: 36–49.

Alattas H, Glick BR, Murphy DV, Scott C. 2024. Harnessing *Pseudomonas* spp. for sustainable plant crop protection. *Frontiers in Microbiology* **15**: 1–21.

Alexou M, Peuke AD. 2013. Chapter 13 methods for xylem sap collection. *Plant Mineral Nutrients* **953**: 195–207.

Allsup CM, George I, Lankau RA. 2023. Shifting microbial communities can enhance tree tolerance to changing climates. *Science* **380**: 835–840.

Almeida RPP, Pereira EF, Purcell AH, Lopes JRS. 2001. Multiplication and movement of a citrus strain of *Xylella fastidiosa* within sweet orange. *Plant Disease* **85**: 382–386.

Andreote FD, Lacava PT, Gai CS, Araújo WL, Maccheroni W, Van Overbeek LS, Van Elsas JD, Azevedo JL. 2006. Model plants for studying the interaction between *Methylobacterium mesophilicum* and *Xylella fastidiosa*. *Canadian Journal of Microbiology* **52**: 419–426.

Anguita-Maeso M, Olivares-García C, Haro C, Imperial J, Navas-Cortés JA, Landa BB. 2020. Culture-dependent and culture-independent characterization of the olive xylem microbiota: effect of sap extraction methods. *Frontiers in Plant Science* **10**: 1–14.

Anguita-Maeso M, Trapero-Casas JL, Olivares-García C, Ruano-Rosa D, Palomo-Ríos E, Jiménez-Díaz RM, Navas-Cortés JA, Landa BB. 2021. *Verticillium dahliae* inoculation and *in vitro* propagation modify the xylem microbiome and disease reaction to *Verticillium* wilt in a wild olive genotype. *Frontiers in Plant Science* **12**: 1–15.

Anzalone A, Di Guardo M, Bella P, Ghadamgahi F, Dimaria G, Zago R, Cirvilleri G, Catara V. 2021. Bioprospecting of beneficial bacteria traits associated with tomato root in greenhouse environment reveals that sampling sites impact more than the root compartment. *Frontiers in Plant Science* **12**: 1–17.

Araújo WL, Marcon J, Maccheroni W, Van Elsas JD, Van Vuurde JWL, Azevedo JL. 2002. Diversity of endophytic bacterial populations and their interaction with *Xylella fastidiosa* in citrus plants. *Applied and Environmental Microbiology* **68**: 4906–4914.

Azevedo JL, Araújo WL, Lacava PT. 2016. The diversity of citrus endophytic bacteria and their interactions with *Xylella fastidiosa* and host plants. *Genetics and Molecular Biology* **39**: 476–491.

Baccari C, Antonova E, Lindow S. 2019. Biological control of Pierce's disease of grape by an endophytic bacterium. *Phytopathology* **109**: 248–256.

Backer R, Rokem JS, Ilangumaran G, Lamont J, Praslickova D, Ricci E, Subramanian S, Smith DL. 2018. Plant growth-promoting rhizobacteria: Context, mechanisms of action, and roadmap to commercialization of biostimulants for sustainable agriculture. *Frontiers in Plant Science* **871**: 1–17.

Baldan E, Nigris S, Romualdi C, D'Alessandro S, Clocchiatti A, Zottini M, Stevanato P, Squartini A, Baldan B. 2015. Beneficial bacteria isolated from grapevine inner tissues shape *Arabidopsis thaliana* roots. *PLoS One* **10**: 1–18.

Bell CR, Dickie GA, Harvey WLG, Chan JWYF. 1995. Endophytic bacteria in grapevine. *Canadian Journal of Microbiology* **41**: 46–53.

Blin K, Shaw S, Augustijn HE, Reitz ZL, Biermann F, Alanjary M, Fetter A, Terlouw BR, Metcalf WW, Helfrich EJN *et al.* 2023. AntiSMASH 7.0: new and improved predictions for detection, regulation, chemical structures and visualisation. *Nucleic Acids Research* **51**: W46–W50.

Bragard C, Dehnen-Schmutz K, Di Serio F, Gonthier P, Jacques MA, Jaques Miret JA, Justesen AF, MacLeod A, Magnusson CS, Milonas P *et al.* 2019a. Effectiveness of *in planta* control measures for *Xylella fastidiosa*. *EFSA Journal* **17**.

Bragard C, Dehnen-Schmutz K, Di Serio F, Gonthier P, Miret JAJ, Justesen AF, Macleod A, Magnusson CS, Milonas P, Navas-Cortes JA *et al.* 2019b. Pest categorisation of the ralstonia solanacearum species complex. *EFSA Journal* **17**: 28.

Casarin N, Hasbroucq S, Carestia G, Glibert A, Bragard C, Grégoire JC. 2023. Investigating dispersal abilities of *Aphrophoridae* in European temperate regions to assess the threat of potential *Xylella fastidiosa*-based pathosystems. *Journal of Pest Science* **96**: 471–488.

Casarin N, Hasbroucq S, Pesenti L, Géradin A, Emond A, López-Mercadal J, Miranda MÁ, Grégoire J-C, Bragard C. 2022. *Salicaceae* as potential host plants of *Xylella fastidiosa* in European temperate regions. *European Journal of Plant Pathology* **165**: 489–507.

Chatterjee S, Wistrom C, Lindow SE. 2008. A cell-cell signaling sensor is required for virulence and insect transmission of *Xylella fastidiosa*. *Proceedings of the National Academy of Sciences, USA* **105**: 2670–2675.

Cheng G, Cheng Y, Rahman E. 2023. Diversity analysis of *Populus euphratica* endophytic bacteria in Tarim River Basin, China. *PeerJ* **11**: 1–18.

Choi KH, Schweizer HP. 2006. mini-Tn7 insertion in bacteria with single attTn7 sites: example *Pseudomonas aeruginosa*. *Nature Protocols* **1**: 153–161.

Cochard H, Casella E, Mencuccini M. 2007. Xylem vulnerability to cavitation varies among poplar and willow clones and correlates with yield. *Tree Physiology* **27**: 1761–1767.

Collazo C, Abadias M, Aguiló-Aguayo I, Alegre I, Chenoll E, Viñas I. 2017. Studies on the biocontrol mechanisms of *Pseudomonas graminis* strain CPA-7 against food-borne pathogens *in vitro* and on fresh-cut melon. *LWT – Food Science and Technology* **85**: 301–308.

Compant S, Cassan F, Kostić T, Johnson L, Brader G, Trognitz F, Sessitsch A. 2024. Harnessing the plant microbiome for sustainable crop production. *Nature Reviews Microbiology* **23**: 9–23.

Compant S, Duffy B, Nowak J, Clément C, Barka EA. 2005a. Use of plant growth-promoting bacteria for biocontrol of plant diseases: Principles, mechanisms of action, and future prospects. *Applied and Environmental Microbiology* **71**: 4951–4959.

Compant S, Reiter B, Sessitsch A, Nowak J, Clément C, Barka EA. 2005b. Endophytic colonization of *Vitis vinifera* L. by plant growth-promoting bacterium *Burkholderia* sp. strain PsJN. *Applied and Environmental Microbiology* **71**: 1685–1693.

Cruz LF, Cobine PA, De La Fuente L. 2012. Calcium increases *Xylella fastidiosa* surface attachment, biofilm formation, and twitching motility. *Applied and Environmental Microbiology* **78**: 1321–1331.

Das R, Saikia K, Sarma PP, Devi R, Thakur D. 2024. Evaluating the potential of *Bacillus* isolates for chlorpyrifos degradation and their role in tea growth promotion and suppression of pathogens. *Current Microbiology* **81**: 1–13.

De La Fuente L, Merfa MV, Cobine PA, Coleman JJ. 2022. Pathogen adaptation to the xylem environment. *Annual Review of Phytopathology* **60**: 163–186.

Deyett E, Rolshausen PE. 2020. Endophytic microbial assemblage in grapevine. *FEMS Microbiology Ecology* **96**: 1–11.

Di Y, Kui L, Singh P, Feng LL, Yan XL, Lian HL, Sheng LF. 2023. Identification and characterization of *Bacillus subtilis* B9: A diazotrophic plant growth-promoting endophytic bacterium isolated from sugarcane root. *Journal of Plant Growth Regulation* **42**: 1720–1737.

Doty SL, Joubert PM, Firrincieli A, Sher AW, Tournay R, Kill C, Parikh SS, Okubara P. 2023. Potential biocontrol activities of populus endophytes against several plant pathogens using different inhibitory mechanisms. *Pathogens* **12**: 1–20.

Elsharawy AA, Eid NA, Ebrahiem AMY. 2023. Effectiveness of *Bacillus pseudomycoides* strain for biocontrol of early blight on tomato plants. *International Journal of Phytopathology* **12**: 313–325.

EPPO. 2019. PM 7/24 (4) *Xylella fastidiosa*. *EPPO Bulletin* **49**: 175–227.

Faddetta T, Abbate L, Alibrandi P, Arancio W, Siino D, Strati F, De Filippo C, Fatta Del Bosco S, Carimi F, Puglia AM *et al.* 2021. The endophytic microbiota of Citrus limon is transmitted from seed to shoot highlighting differences of bacterial and fungal community structures. *Scientific Reports* **11**: 1–12.

Felipe V, Bianco MI, Terrestre M, Mielnichuk N, Romero AM, Yaryura PM. 2021. Biocontrol of tomato bacterial spot by novel *Bacillus* and *Pseudomonas* strains. *European Journal of Plant Pathology* **160**: 935–948.

Filho ASF, Quecine MC, Bogas AC, de Rossetto PB, de Lima AOS, Lacava PT, Azevedo JL, Araújo WL. 2012. Endophytic *Methylobacterium extorquens* expresses a heterologous β-1,4-endoglucanase A (EglA) in *Catharanthus roseus seedlings*, a model host plant for *Xylella fastidiosa*. *World Journal of Microbiology and Biotechnology* **28**: 1475–1481.

Firrincieli A, Khorasani M, Frank AC, Doty SL. 2020. Influences of climate on phyllosphere endophytic bacterial communities of wild poplar. *Frontiers in Plant Science* **11**: 1–13.

Gai CS, Lacava PT, Quecine MC, Auriac MC, Lopes JRS, Araújo WL, Miller TA, Azevedo JL. 2009. Transmission of *Methylobacterium mesophilicum* by *Bucephalogonia xanthophis* for paratransgenic control strategy of Citrus variegated chlorosis. *Journal of Microbiology* **47**: 448–454.

Gardner JM, Feldman AW, Zablotowicz RM. 1982. Identity and behavior of xylem-residing bacteria in rough lemon roots of Florida citrus trees. *Applied and Environmental Microbiology* **43**: 1335–1342.

Giampetruzzi A, Baptista P, Morelli M, Cameirão C, Neto TL, Costa D, D'attoma G, Kubaa RA, Altamura G, Saponari M *et al.* 2020. Differences in the endophytic microbiome of olive cultivars infected by *Xylella fastidiosa* across seasons. *Pathogens* **9**: 1–29.

Guleria I, Kumari A, Lacaille-Dubois MA, Saini AK, Kumar V, Saini RV, Lal UR, Gaur NA, Kumari S, Seth A *et al.* 2022. In-vitro antimicrobial, antioxidant, anti-inflammatory, and cytotoxic activities of *Populus ciliata* bark and leaves: a comparative study. *South African Journal of Botany* **148**: 238–250.

Haas D, Défago G. 2005. Biological control of soil-borne pathogens by fluorescent Pseudomonads. *Nature Reviews Microbiology* **3**: 307–319.

Hardoim PR, van Overbeek LS, Berg G, Pirttilä AM, Compant S, Campisano A, Döring M, Sessitsch A. 2015. The hidden world within plants: ecological and evolutionary considerations for defining functioning of microbial endophytes. *Microbiology and Molecular Biology Reviews* **79**: 293–320.

Hasan N, Farzand A, Heng Z, Khan IU, Moosa A, Zubair M, Na Y, Ying S, Canming T. 2020. Antagonistic potential of novel endophytic *Bacillus strains* and mediation of plant defense against verticillium wilt in upland cotton. *Plants* **9**: 1–16.

Hauben L, Steenackers M, Swings J. 1998. PCR-based detection of the causal agent of watermark disease in willows (*Salix* spp.). *Applied and Environmental Microbiology* **64**: 3966–3971.

Hill BL, Purcell AH. 1995. Multiplication and movement of *Xylella fastidiosa* within grapevine and four other plants. *Phytopathology* **85**: 1368–1372.

Huang CJ, Wang TK, Chung SC, Chen CY. 2005. Identification of an antifungal chitinase from a potential biocontrol agent, *Bacillus cereus* 28-9. *Journal of Biochemistry and Molecular Biology* **38**: 82–88.

Huang H, Hsieh T, Erickson R. 2003. Biology and epidemiology of *Erwinia rhapontici*, causal agent of pink seed and crown rot of plants. *Plant Pathology Bulletin* **12**: 69–76.

Köhl J, Kolnaar R, Ravensberg WJ. 2019. Mode of action of microbial biological control agents against plant diseases: relevance beyond efficacy. *Frontiers in Plant Science* **10**: 1–19.

Lacava PT, Araújo WL, Marcon J, Maccheroni W, Azevedo JL. 2004. Interaction between endophytic bacteria from citrus plants and the phytopathogenic bacteria *Xylella fastidiosa*, causal agent of citrus-variegated chlorosis. *Letters in Applied Microbiology* **39**: 55–59.

Lacava PT, Li W, Araújo WL, Azevedo JL, Hartung JS. 2007. The endophyte *Curtobacterium flaccumfaciens* reduces symptoms caused by *Xylella fastidiosa* in *Catharanthus roseus*. *Journal of Microbiology* **45**: 388–393.

Lengrand S, Dubois B, Renoz F, Lebbe O. 2025. Seed-borne endophytic bacteria of tomato – dynamic colonization and implication in plant health. *Phytobiomes Journal* **0**: 1–67.

Lengrand S, Pesenti L, Bragard C, Legrève A. 2024. Bacterial endophytome sources, profile and dynamics – a conceptual framework. *Frontiers in Sustainable Food Systems* **8**: 1–16.

Lindow S, Koutsoukis R, Meyer K, Baccari C. 2024. Control of Pierce's disease of grape with *Paraburkholderia phytofirmans* PsJN in the field. *Phytopathology* **114**: 503–511.

Liu B, Zheng D, Zhou S, Chen L, Yang J. 2022. VFDB 2022: a general classification scheme for bacterial virulence factors. *Nucleic Acids Research* **50**: D912–D917.

Loper JE, Hassan KA, Mavrodi DV, Davis EW, Lim CK, Shaffer BT, Elbourne LDH, Stockwell VO, Hartney SL, Breakwell K *et al.* 2012. Comparative genomics of plant-associated *Pseudomonas* spp.: Insights into diversity and inheritance of traits involved in multitrophic interactions. *PLoS Genetics* **8**: e1002784.

Louden BC, Haarmann D, Lynne AM. 2011. Use of blue agar CAS assay for siderophore detection. *Journal of Microbiology & Biology Education* **12**: 51–53.

Maes M, Huvenne H, Messens E. 2009. *Brenneria salicis*, the bacterium causing watermark disease in willow, resides as an endophyte in wood. *Environmental Microbiology* **11**: 1453–1462.

Marques LLR, Ceri H, Manfio GP, Reid DM, Olson ME. 2002. Characterization of biofilm formation by *Xylella fastidiosa in vitro*. *Plant Disease* **86**: 633–638.

Martínez-Hidalgo P, García JM, Pozo MJ. 2015. Induced systemic resistance against *Botrytis cinerea* by *Micromonospora* strains isolated from root nodules. *Frontiers in Microbiology* **6**: 1–11.

Meier-Kolthoff JP, Auch AF, Klenk HP, Göker M. 2013. Genome sequence-based species delimitation with confidence intervals and improved distance functions. *BMC Bioinformatics* **14**: 1–14.

Mikiciński A, Sobiczewski P, Puławska J, Maciorowski R. 2016. Control of fire blight (*Erwinia amylovora*) by a novel strain 49M of *Pseudomonas graminis* from the phyllosphere of apple (*Malus* spp.). *European Journal of Plant Pathology* **145**: 265–276.

Moriya Y, Itoh M, Okuda S, Yoshizawa AC, Kanehisa M. 2007. KAAS: an automatic genome annotation and pathway reconstruction server. *Nucleic Acids Research* **35**: 182–185.

Mourou M, Hanani A, D'onghia AM, Davino SW, Balestra GM, Valentini F. 2022. Antagonism and antimicrobial capacity of epiphytic and endophytic bacteria against the phytopathogen *Xylella fastidiosa*. *Agronomy* **12**: 1–12.

Newman KL, Almeida RPP, Purcell AH, Lindow SE. 2003. Use of a green fluorescent strain for analysis of *Xylella fastidiosa* colonization of *Vitis vinifera*. *Applied and Environmental Microbiology* **69**: 7319–7327.

Nicotra D, Ghadamgahi F, Ghosh S, Anzalone A, Dimaria G, Mosca A, Massimino ME, Vetukuri RR, Catara V. 2024. Genomic insights and biocontrol potential of ten bacterial strains from the tomato core microbiome. *Frontiers in Plant Science* **15**: 1–23.

O'Toole GA. 2010. Microtiter dish Biofilm formation assay. *Journal of Visualized Experiments* **47**: 10–11.

Ogata H, Goto S, Sato K, Fujibuchi W, Hidemasa B, Kanehisa M. 1999. KEGG: Kyoto encyclopedia of genes and genomes. *Oxford University Press* **27**: 29–34.

Ongena M, Jourdan E, Adam A, Paquot M, Brans A, Joris B, Arpigny JL, Thonart P. 2007. Surfactin and fengycin lipopeptides of *Bacillus subtilis* as elicitors of induced systemic resistance in plants. *Environmental Microbiology* **9**: 1084–1090.

Patz S, Gautam A, Becker M, Ruppel S, Rodríguez-Palenzuela P, Huson DH. 2021. PLaBAse: a comprehensive web resource for analyzing the plant growth-promoting potential of plant-associated bacteria. *bioRxiv*.

Paul D, Sinha SN. 2017. Isolation and characterization of phosphate solubilizing bacterium *Pseudomonas aeruginosa* KUPSB12 with antibacterial potential from river Ganga, India. *Annals of Agrarian Science* **15**: 130–136.

Pesenti L. 2024. Bacterial threat to willows: understanding the epidemiology of *Brenneria salicis*. *Cabi Plant Health Case* **29**: 1–8.

Pesenti L. 2025. Managing *Xylella fastidiosa* in Europe: exploring biocontrol strategies. *Cabi Plant Health Case* **9**: 1–16.

Pieterse CMJ, Zamioudis C, Berendsen RL, Weller DM, Van Wees SCM, Bakker PAHM. 2014. Induced systemic resistance by beneficial microbes. *Annual Review of Phytopathology* **52**: 347–375.

Poppe L, Vanhoutte S, Höfte M. 2003. Modes of action of *Pantoea agglomerans* CPA-2, an antagonist of postharvest pathogens on fruits. *European Journal of Plant Pathology* **109**: 963–973.

Purcell AH, Hopkins DL. 1996. Fastidious xylem-limited bacterial plant pathogens. *Annual Review of Phytopathology* **34**: 131–151.

Raaijmakers JM, Mazzola M. 2012. Diversity and natural functions of antibiotics produced by beneficial and plant pathogenic bacteria. *Annual Review of Phytopathology* **50**: 403–424.

Rabbee MF, Hwang BS, Baek KH. 2023. *Bacillus velezensis*: A beneficial biocontrol agent or facultative phytopathogen for sustainable agriculture. *Agronomy* **13**: 1-14.

Rigo GV, Cardoso FG, Galego GB, Rosa DF, Santos ALS, Tasca T. 2023. Metallopeptidases as key virulence attributes of clinically relevant protozoa: new discoveries, perspectives, and frontiers of knowledge. *Current Protein & Peptide Science* **24**: 307–328.

Santoyo G. 2022. How plants recruit their microbiome? New insights into beneficial interactions. *Journal of Advanced Research* **40**: 45–58.

Santoyo G, Moreno-Hagelsieb G, del Carmen Orozco-Mosqueda M, Glick BR. 2016. Plant growth-promoting bacterial endophytes. *Microbiological Research* **183**: 92–99.

Shahzad A, Aslam U, Ferdous S, Qin M, Siddique A, Billah M, Naeem M, Mahmood Z, Kayani S. 2024. Combined effect of endophytic *Bacillus mycoides* and rock phosphate on the amelioration of heavy metal stress in wheat plants. *BMC Plant Biology* **24**: 1–16.

Shen Q, Zhou H, Dai G, Zhong G, Huo L, Li A, Liu Y, Yang M, Ravichandran V, Zheng Z *et al.* 2022. Characterization of a cryptic NRPS gene cluster in *Bacillus velezensis* FZB42 reveals a discrete oxidase involved in multithiazole biosynthesis. *ACS Catalysis* **12**: 3371–3381.

Slama H, Cherif-Silini H, Bouket AC, Qader M, Silini A, Yahiaoui B, Alenezi FN, Luptakova L, Triki MA, Vallat A *et al.* 2019. Screening for fusarium antagonistic bacteria from contrasting niches designated the endophyte *Bacillus halotoleransas* plant warden against *Fusarium*. *Frontiers in Microbiology* **10**: 1–24.

Sorokan A, Gabdrakhmanova V, Kuramshina Z, Khairullin R, Maksimov I. 2023. Plant-associated *Bacillus thuringiensis* and *Bacillus cereus*: inside agents for biocontrol and genetic recombination in Phytomicrobiome. *Plants* **12: 1-24**.

Taghavi S, Barac T, Greenberg B, Borremans B, Vangronsveld J, Van Der Lelie D. 2005. Horizontal gene transfer to endogenous endophytic bacteria from poplar improves phytoremediation of toluene. *Applied and Environmental Microbiology* **71**: 8500–8505.

Taghavi S, van der Lelie D, Hoffman A, Zhang YB, Walla MD, Vangronsveld J, Newman L, Monchy S. 2010. Genome sequence of the plant growth promoting endophytic bacterium *Enterobacter* sp. 638. *PLoS Genetics* **6**: 19.

Thomas P, Shaik SP. 2020. Molecular profiling on surface-disinfected tomato seeds reveals high diversity of cultivation-recalcitrant endophytic bacteria with low shares of spore-forming firmicutes. *Microbial Ecology* **79**: 910–924.

Thomloudi EE, Tsalgatidou PC, Baira E, Papadimitriou K, Venieraki A, Katinakis P. 2021. Genomic and metabolomic insights into secondary metabolites of the novel bacillus halotolerans hil4, an endophyte with promising antagonistic activity against gray mold and plant growth promoting potential. *Microorganisms* **9**: 1–32.

Tilley D, Law R, Warren S, Samis JA, Kumar A. 2014. CpaA a novel protease from *Acinetobacter baumannii* clinical isolates deregulates blood coagulation. *FEMS Microbiology Letters* **356**: 53–61.

Turner JG, Davis JML, Guven K. 1992. Watermark disease of tree willows. *Proceedings – Royal Society of Edinburgh, Section B* **98B**: 105–117.

Urusova DV, Kinsella RL, Salinas ND, Haurat MF, Feldman MF, Tolia NH. 2019. The structure of *Acinetobacter*-secreted protease CpaA complexed with its chaperone CpaB reveals a novel mode of a T2SS chaperone-substrate interaction. *Journal of Biological Chemistry* **294**: 13344–13354.

Vinatzer BA. 2012. 'Listening in' on how a bacterium takes over the plant vascular system. *MBio* **3**: 8–9.

Walsh UF, Morrissey JP, O'Gara F. 2001. *Pseudomonas* for biocontrol of phytopathogens: from functional genomics to commercial exploitation. *Current Opinion in Biotechnology* **12**: 289–295.

Wang H, Xin J, Zhang X, Jiang S. 2025. Identification and functional analysis of endophytic bacteria *Bacillus cereus* in *Sphagnum palustre*. *Plants* **14**: 1–21.

Wang H, Zhang F, Zhang Y, Wang M, Zhang Y, Zhang J. 2024. Enrichment of novel entomopathogenic *Pseudomonas* species enhances willow resistance to leaf beetles. *Microbiome* **12**: 169.

Wang WY, Kong WL, Liao YCZ, Zhu LH. 2022. Identification of *Bacillus velezensis* SBB and its antifungal effects against *Verticillium dahliae*. *Journal of Fungi* **8**: 1–18.

Weisburg WG, Barns SM, Pelletier DA, Lane DJ. 1991. 16S ribosomal DNA amplification for phylogenetic study. *Journal of Bacteriology* **173**: 697–703.

Wu JJ, Huang JW, Deng WL. 2020. Phenylacetic acid and methylphenyl acetate from the biocontrol bacterium *Bacillus mycoides* BM02 suppress spore germination in *Fusarium oxysporum* f. sp. *lycopersici*. *Frontiers in Microbiology* **11**: 1–12.

Yadeta KA, Thomma BPHJ. 2013. The xylem as battleground for plant hosts and vascular wilt pathogens. *Frontiers in Plant Science* **4**: 1–12.

Yoon SH, Min HS, E Lim J, Kwon S, Chun J. 2017. A large-scale evaluation of algorithms to calculate average nucleotide identity. *Antonie van Leeuwenhoek International Journal of General and Molecular Microbiology* **110**: 1281–1286.

Zhang L, Khabbaz SE, Wang A, Li H, Abbasi PA. 2015. Detection and characterization of broad-spectrum antipathogen activity of novel rhizobacterial isolates and suppression of *Fusarium* crown and root rot disease of tomato. *Journal of Applied Microbiology* **118**: 685–703.

Zhang P, Hao H, Wang L, Liu Z, Ma L. 2022. Endophytes *Bacillus amyloliquefaciens* AW3 (CGMCC1.16683) improves the growth of *Populus davidiana* × *Populus bolleana* (PdPap) and induces its resistance to wilt disease by *Fusarium oxysporum* Fox68 (CFCC86068). *European Journal of Plant Pathology* **162**: 1–17.

Zhong X, Jin Y, Ren H, Hong T, Zheng J, Fan W, Zhong K, Huang G. 2024. Research progress of *Bacillus velezensis* in plant disease resistance and growth promotion. *Frontiers in Industrial Microbiology* **2**: 1–11.

Zhou F, Emonet A, Dénervaud Tendon V, Marhavy P, Wu D, Lahaye T, Geldner N. 2020. Co-incidence of damage and microbial patterns controls localized immune responses in roots. *Cell* **180**: 440–453.

Zicca S, De Bellis P, Masiello M, Saponari M, Saldarelli P, Boscia D, Sisto A. 2020. Antagonistic activity of olive endophytic bacteria and of *Bacillus* spp. strains against *Xylella fastidiosa*. *Microbiological Research* **236**: 126467.

Supporting Information

Additional Supporting Information may be found online in the Supporting Information section at the end of the article.

Fig. S1 Plasmid maps of constructs used to tag endophytic bacterial strains and corresponding primer binding sites for *in planta* detection.

Fig. S2 Standard curves for quantitative polymerase chain reaction detection of bacterial strains and plant reference gene. Calibration curves were generated for each inoculated bacterial strain and for the tobacco plant reference gene β-tubulin to enable absolute quantification of bacterial load *in planta*.

Fig. S3 Bacterial isolates present in xylem sap of different *Salicaceae* species from willow (framed in blue) and poplar (framed in orange) genera extracted with Scholander pressure chamber respective of culture medium used (BCYE, KB, PDA, TSA).

Fig. S4 Relative abundance of the top 10 most abundant bacterial genera (1) and species (2) isolated from *Salicaceae*, based on 16S rRNA sequencing.

Fig. S5 Relative abundances of plant and bacteria in xylem sap of *S. alba* (89–94), *S. caprea* (95–100), *P. canescens* (101–106), *P. tremula* (107–112) as determined by Illumina sequencing using two PCR-primer pairs (V1V3 and V3V4).

Fig. S6 Richness, Shannon diversity indices at ASVs' taxonomic level determined. Dots represent the values for all samples tested in each PCR-primer pair and each plant species.

Fig. S7 Number of orthologous clusters in each species and shared orthologous gene clusters among species.

Fig. S8 Percentage of genes encoding for PGPT (Patz *et al.*, 2021). Factor categories are specified on the left. Strain ID is indicated in the bottom.

Fig. S9 Percentage of genes encoding for 'plant bacterial only interaction factors (proteins)' predicted through PIFAR-BASE (Patz *et al.*, 2021). Factor categories are specified on the left. Strain ID is indicated in the bottom.

Fig. S10 Verification of plasmid integration in fluorescently transformed endophytic bacteria. PCR amplification of fluorescent gene markers confirms the successful transformation of *Brenneria salicis* LMG2698, *Erwinia rhapontici* 11–25, *Pseudomonas coleopterorum* 9–161, and *Pseudomonas graminis* 9–169.

Fig. S11 Inoculation of endophyte alone – Growth indexes for *N. tabacum* (A) and *S. caprea in vitro* plantlets (B) inoculated with different endophytic bacteria.

Fig. S12 One-month co-inoculation assay in tobacco plants.

Fig. S13 Three-month co-inoculation assay in tobacco plants.

Fig. S14 Three-month co-inoculation assay in tobacco plants.

Fig. S15 One-month co-inoculation assay in willow.

Fig. S16 Three-month co-inoculation assay in willow Endophyte Cq in plant tissue.

Fig. S17 Three-month co-inoculation assay in willow.

Fig. S18 Confocal microscopy images of inoculated plant samples.

Table S1 Primers list and sequences for PCR transformation validation and detection *in planta*.

Table S2 Primers list and sequences for quantitative polymerase chain reaction detection *in planta*.

Table S3 Mean bacterial species richness and Shannon diversity index for each *Salicaceae* host species based on culture-dependent isolation from xylem sap.

Table S4 General features of the genomic assembly of the 15 endophytic bacterial strains selected.

Table S5 Functional distribution of predicted KEGG metabolic pathways in the genomes of sequenced *Bacillus*, *Pseudomonas*, and *Erwinia* strains.

Table S6 Description of secondary metabolite BGCs found in the genome of endophytic bacterial strains.

Table S7 Distribution of putative virulence and biocontrol-associated genes in the genomes of Bacillus and Pseudomonas strains, as identified using the Virulence Factor Database (VFDB).

Table S8 Inhibition in confrontation *in vitro* of pathogenic strains by endophytic bacteria.

Table S9 Detection and re-isolation of endophytic strains following single inoculation in *Nicotiana tabacum* and *Salix caprea in vitro* plantlets.

Table S10 Average of bacterial concentration at Tf expressed in potential CFU/g of plant tissue determined by qPCR after the generation of a standard calibration for Control group with endophyte (A), then for *X. fastidiosa*-inoculated group (B) and then for *B. salicis* inoculates group (C).

Please note: Wiley is not responsible for the content or functionality of any Supporting Information supplied by the authors. Any queries (other than missing material) should be directed to the *New Phytologist* Central Office.

Disclaimer: The New Phytologist Foundation remains neutral with regard to jurisdictional claims in maps and in any institutional affiliations.